G0S2 impairs ATGL activity and cell cycle progression in murine liver

A dissertation submitted to the Faculty of Medicine in partial fulfilment of the requirements for the degree of

"Doctor in human biology" (Dr. Hum. Biol.)

By

Sundaram Reddy Chakkarappan

Podattur Pet

December 2012

Institute of Molecular Medicine

Max-Planck Research Group on Stem Cell Ageing

University of Ulm

Declaration

Herewith, I confirm that I have written the present PhD thesis myself and independently and used no other aids than those cited. In each individual case, I have clearly identified the source of the passages that are taken word for word or paraphrased from other works.

I also hereby declare that I have carried out my scientific work according to the principles of good scientific practice in accordance with the current 'Satzung der Universität Ulm zur Sicherung guter wissenschaftlicher Praxis'

Ulm, December 2012

Sundaram Reddy Chakkarappan

Dean: Prof. Dr. Thomas Wirth

1. Prof. dr. Karl Lenhard Rudolph
2. Prof. dr. Martin wabitsch
3. PD. Dr. Cagatay Günes
4. PD. Dr. Mathias Dollinger

Date of thesis defense: 19.04.2013

Table of contents

Abbreviations……6

Abstract……..8

1. Introduction…….9

1.1 Overview of Triglyceride Metabolism……...9

1.2 G0/G1 Switch Regulatory Protein 2……11

1.3 G0S2 functions as a Tumor Suppressor Gene……11

1.4 G0S2, a Pro-apoptotic Factor……...12

1.5 G0S2 is a PPAR Target gene……12

1.6 Regulation of Adipose Triglyceride Lipase by G0S2…….13

1.7 Regulation of Lipolysis by G0S2……..16

1.8 G0S2, Regulator of Cell Cycle…….18

1.9 Liver Regeneration……...18

1.10 Aim of the work…….19

2. Material and Methods……..20

2.1 Laboratory equipment……..21

2.2 Softwares……21

2.3 Chemicals and Biochemicals……22

2.4 Animal work……..23

2.4.1 Generation of G0s2 Straight Knockout Mouse……..23

2.4.2 Primers for Genotyping and RT-PCR……24

2.4.3 Maintenance and Handling of Animals……..24

2.5 Immunohistochemistry…….24

2.5.1 Processing of Tissue……..24

2.5.2 Immunohistochemistry Staining For Tissues…….25

2.6 Protein analysis…….25

2.6.1 Protein Isolation and Concentration Measurement……..25

2.6.2 Western Blotting……...26

2.7 RNA Analysis…….26

2.7.1 RNA Isolation……26

2.7.2 DNase I Treatment……27

2.7.3 cDNA Synthesis…….27

2.7.4 Quantitative Real Time PCR and Microarray……...27

2.8 Fat Measurement……..28

2.8.1 In vitro Adipogenesis Assay…….28

2.8.2 High Fat Diet…….28

2.8.3 Fat Staining and Triglyceride Quantification……28

2.8.4 Assay for Triglyceride Hydrolase Activity…….29

2.8.5 Growth Curve……30

2.8.6 Partial Hepatectomy (PH)……30

2.9 Southern Blot Analysis…….30

2.9.1 Genomic DNA Isolation from Tissue……..30

2.9.2 Southern Blot Analysis for G0S2…….31

2.10 FACS Analysis……...32

2.10.1 Bone Marrow……32

3. Results……34

3.1 Generation of G0S2 knockout mouse……..35

3.2 G0S2 deletion does not induce apoptosis……38

3.3 G0S2 is dispensable for adipogenesis both in cell culture and *in vivo*….40

3.4 G0S2 deletion does not induce lipolysis in white adipose tissue……...42

3.5 G0S2 deletion improves liver regeneration after starvation…….47

3.6 Fat deposition in liver is reduced in G0S2 knockout mice……49

3.7 Enhanced ATGL Activity Is Associated With Improved Liver……...53

3.8 G0S2 inhibits cell cycle after starvation……..54

4. Discussion……...57

5. References……..66

6. Acknowledgements……75

7. Curriculum vitae……...77

Abbreviations

aa	amino acids
ATP	adenosine triphosphate
ATGL	adipose triglyceride lipase
bp	base pairs
cDNA	complementary DNA
CGI-8	comparative gene identification 8
DMEM	Dulbecco's Modified Eagle Medium
DMSO	dimethyl sulfoxide
DNA	deoxyribonucleic acid
dNTP	deoxynucleotide triphosphate
EDTA	ethylenediaminetetraacetate
FACS	fluorescence activated cell sorting
FBS	fetal bovine serum
FITC	fluorescein isothiocyanate
g	gram
GFP	green fluorescent protein
G0s2	G0/G1 switch gene 2
Gy	gray (unit)
h	hour(s)
HF	high fat
HRP	horse radish peroxidase
HSL	hormone sensitive lipase
HSCs	heamatopoietic stem cells
IgG	immunoglobulin G
IR	ionizing radiation
kb	kilo bases
kDa	kilo Dalton
L	liter
min	minute(s)
mRNA	messenger RNA
n.a.	not available

n.d.	not determined
ND	normal diet
n.s.	not significant
nm	nano meter
nt	nucleotides
OGTT	oral glucose tolerance test
PBS	phosphate buffered saline
PC7	PE-Cy7
PCR	polymerase chain reaction
PE	phycoerythrin
PH	partial hepatectomy
PI3K	phosphatidylinositol 3-kinase
PMSF	phenylmethylsulfonyl fluoride
PVDF	polyvinylidene fluoride
qRT-PCR	quantitative real time polymerase chain reaction
RT-PCR	reverse transcriptase polymerase chain reaction
RNA	ribonucleic acid
sec	second(s)
SEM	standard error mean
UTR	untranslated region
V	volt
wt	wildtype

Abstract

The G0/G1 switch gene 2 (G*0s2*) has putative roles in cellular proliferation and fat metabolism. While activated blood mononuclear cells increase the expression of G0S2, cancer cells silence it by promoter methylation. Moreover, G0S2 was shown to act as a proapoptotic factor and recently as an inhibitor of the adipose triglyceride lipase (ATGL) in cell cuture studies. Nonetheless, the role of G0S2 in an *in vivo* setting remains elusive. Here I describe the characterization of a novel *G0s2* knockout mouse model. *G0s2* knockout mice are born at expected mendelian ratio and develop normally under normal and high fat diet feeding conditions. Liver regeneration is improved in mice with *G0s2* deletion under starvation conditions. Improved cell cycle re-entry in *G0s2* knockout livers after partial hepatectomy is associated with decreased triglyceride deposition and lipid droplet formation after 20h of starvation. Supporting the notion of G0S2 acting as a cell cycle inhibitor under certain conditions, over-expression of G0S2 in the hematopoietic system improves stem cell function and hematopoietic reconstitution by maintaining stem cell quiescence and inhibiting their depletion during serial transplantation. This data suggests that G0S2 has cell-cycle regulatory functions in liver and hematopoietic system possibly involving its role in modulating fat metabolism in mice starvation.

1. Introduction

1. 1 Overview of Triglyceride Metabolism

Triglycerides (TGs) are esters derived from glycerol and three fatty acids, which may be either saturated or unsaturated fatty acids. Triglycerides are mainly stored in adipose tissue and TGs represent a major storage form of energy in mammals (1). TGs are derived from both extracellular and intracellular sources like dietary foods and *de novo* synthesis of TGs in the endoplasmic reticulum of liver and adipose tissue (2).

Figure 1.1 provides the detailed information of TG metabolism during fed state. Dietary fatty acids (FA) are absorbed from the gut and converted to TGs and incorporated into chylomicrons in the intestinal epithelial cells. The TG-rich apolipoprotein B48 (Apo B48) containing chylomicrons enter the plasma via the intestinal lymph (3-5). Lipoprotein lipase (LPL) hydrolyses the triglyceride in chylomicrons to fatty acids, which are taken up by muscle cells for oxidation or adipocytes for storage. The remaining particles, the chylomicron remnants, are removed from the circulation by the liver through binding of their surface ApoE to the low density lipoprotein (LDL) receptor or LDL receptor related protein. Very low density lipoprotein (VLDL) particles are triglyceride-rich apoB100 containing particles, synthesized by the liver. As with chylomicrons, VLDL triglycerides are hydrolyzed by LPL. VLDL remnants or intermediate density lipoproteins (IDL) are taken up by liver receptors via ApoE or converted to LDL. Chylomicrons, VLDL and their respective remnants (6-10) (RLP, remnant lipoproteins) are termed triglyceride-rich lipoproteins (TRL). Under physiological conditions, insulin, which is raised in the postprandial state, suppresses lipolysis from adipose tissue and hepatic VLDL production; however, this insulin action is inappropriate in insulin resistance and type 2 diabetes, resulting in high TRL concentrations. The large

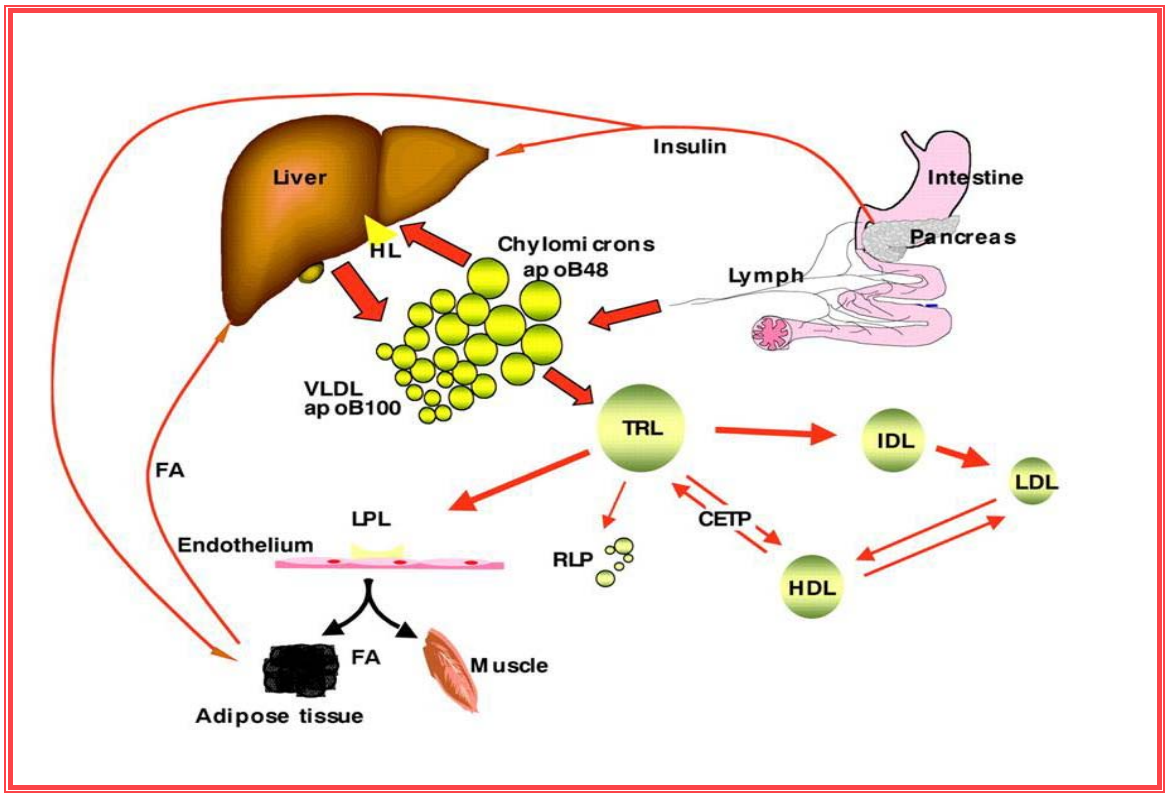

Figure 1.1 Overview of lipid metabolism *in vivo* under fed conditions. Under fed state, insulin and lipoprotein lipase facilitates the transport of triglyceride into adipose tissue for storage with the help of lipoproteins. The fatty acids are used for energy production in muscles and other tissues. Abbreviations: TRL- Triglyceride rich lipoprotein; IDL- Intermediate density lipoprotein; LDL- Low density lipoprotein; HDL- High density lipoprotein; RLP – Remnant lipoprotein; CETP - Cholesteryl ester transfer protein (M E Tushuizen etal (4)).

amount of TRL and their prolonged residence time in the circulation increase the exchange of esterified cholesterol from high density lipoprotein (HDL) and LDL to TRL and of triglycerides to LDL and HDL particles, which is mediated by cholesterol-ester transfer protein (CETP). Triglyceride enrichment of LDL particles renders them better substrates for hepatic lipase (HL), which hydrolyses triglycerides from the core of LDL and turns them into smaller and denser particles. Small dense LDL is more atherogenic as they readily enter the subendothelial space and become oxidised. Triglyceride enriched HDL particles are smaller and are more rapidly catabolized, which may explain the observed low plasma HDL in insulin resistance and type 2 diabetes (11-14).

1.2. G0/G1 Switch Regulatory Protein 2 (G0S2)

G0S2 is known as G0/G1 switch gene 2, a 103 amino acid containing small basic protein located on chromosome 1 of both mouse and human genome. The G0S2 protein is highly conserved and there is a 78% homology between human and mouse isoforms. *G0s2* gene contains two exons, exon 1 contains 5'UTR, and kozak sequence and exon 2 has an open reading frame. The G0S2 protein is mainly located in the mitochondria and endoplasmic reticulum (15, 16). G0S2 is expressed in a BMP-2 dependent manner during embryonic development and its expression is mainly seen in liver, brown and in white adipose tissue (17). The secondary structure of G0S2 has alpha-helical domains separated by a hydrophobic region with the potential to generate turns and assume a beta-sheet conformation (18). *G0s2* gene contains a CpG rich island, suggesting its expression in germ line and G0S2 is a phosphoprotein containing potential phosphorylation sites for protein kinase C, cdc2 and casein kinase II (18, 19). The promoter of the *G0s2* gene contains potential transcription factor biding sites for AP1, AP2, AP3, NFAT and NFkB, which is consistent with the rapid transcriptional activation of *G0s2* in response to activating agents like TNF-α, lectin, retinoic acid (RA), peroxisome proliferator-activated receptors (PPARs), glucose and insulin (20-25).

G0S2 is a member of set of G0s genes, that were initially identified to be expressed in lectin or ConA stimulated cultured human mononuclear cells. It was thought that the suppressed expression of G0S2 in response to ConA treatment is involved in inhibiting the entry of resting cells that are in G0 stage of the cell cycle into the G1 phase of the cell cycle (26).

1.3 G0S2 function as a Tumor Suppressor Gene

Epigenetic changes can lead to abnormal expression of genes in cancer and

several genes have been reported to have aberrant promoter methylation in cancer (27). Whereas anti-cancer agents are used to treat solid tumors, the development of secondary resistance remains a problem to clinical efficacy. Some of the anti-cancer agents like cisplatin mediate DNA hypermethylation thereby inactivating genes required for cytotoxicity (27). *G0s2* is a one of the genes that undergoes hypermethylation in response to cancer treatment (28). A suggestive role of G0S2 as a tumour suppressor was further proposed with the identification of its histone H3 lysine 9 hypermethylation and gene silencing in squamous lung carcinoma and head and neck cancer (29-32).

1.4 G0S2, a Pro-apoptotic Factor

An additional function of G0S2 as a pro-apoptotic factor was suggested as G0S2 binds Bcl-2 proteins directly, although lacking Bcl-2 domains, and promotes apoptosis in a human cancer cell line (15). G0S2 induces apoptosis by directly interacting with Bcl-2 and preventing its ability to heterodimerize with Bax (15).

It was previously shown that *G0s2* gene is epigenetically silenced in number of human cancers whereas knockdown of G0S2 promoted oncogenic transformation (32). The pro-apoptotic activity of G0S2 and its epigenetic silencing in human tumors and in human cancer cell lines raises the possibility that G0S2 is a tumor suppressor gene (32).

1.5 G0S2 is a PPAR Target Gene

PPARs (peroxisome proliferators activated receptors) represent a group of nuclear receptors that play an important role in regulation of energy metabolism (33). There are three different nuclear receptors: PPARα, PPARβ/δ and PPARγ. PPARα is involved in the regulation of fatty acid oxidation in liver (34), whereas PPARγ is a master regulator of adipocyte differentiation in white adipose tissue (35-38) by stimulating genes

involved in lipogenesis like aP2 (adipocyte fatty acid binding protein), lipoprotein lipase and CD36/fatty acid translocase.

Previous studies have shown that by comparing the mRNA levels of wild type and PPARα null mice after 24h fasting, *G0s2* mRNA was upregulated in liver directly by PPARα through binding to PPAR-responsive element in *G0s2* promoter (21, 39).

However, in white adipose tissue G0S2 is mainly regulated by PPARγ (40) as shown by the *in vitro* adipogenesis assay in mouse 3T3-L1 preadipocyte cell lines and human Simpson–Golabi–Behmel syndrome (SGBS) fibroblast cell line (41, 42). Both G0S2 and PPARγ are upregulated during adipogenesis suggesting a link between PPARγ and G0S2 in adipose tissue and G0S2 was shown as a direct target of PPARγ. Previous studies have shown that treatment with PPARγ agonist rosiglitazone significantly increased G0S2 protein in cultured mouse 3T3-L1 preadipocyte cell lines. Activation of PPARγ stimulates its target genes including insulin dependent glucose and fatty acid uptake, TG synthesis and storage, epinephrine stimulated lipolysis, and synthesis and secretion of adipokines (43-47). These studies show that G0S2 could be involved in one or more on adipose tissue functions stimulated by PPARγ. However, G0S2 appears to be regulated by different PPARs in different tissues (48-51).

1.6. Regulation of Adipose Triglyceride Lipase by G0S2

In most organisms excess energy is stored in the form of triacylglycerol (TG) in lipid droplets. During the periods of increasing energy demand conditions like starvation, TG undergoes a hydrolytic process termed lipolysis, which results in the release of free fatty acids (FFAs) and glycerol as energy source (52-55). Adipose triglyceride lipase is the rate limiting enzyme in lipolysis, which acts only on neutral lipids like TG, whereas hormone sensitive lipase is more specific towards diglycerides and monoglyceride

lipase acts on monoglycerides (56, 57).

ATGL, is also known as PNPLA2 (patatin like phospholipase domain containing-2), patients with mutations in these gene develop lipid storage disease with myopathy (58). ATGL is present both in the cytosol and surface of lipid droplets (LD) and ATGL catalyzes the lipolysis through N-terminal portion of ATGL (59) and ATGL is highly expressed in white and brown adipose tissue and liver. The N-terminal region of ATGL contains α/β-hydrolase fold and patatin-like domain which is characterized as a catalytic site similar to that of human cytosolic phospholipase A2 (cPLA2) (60-63). The 45 amino acids in the hydrophobic C-terminal region mediate targeting ATGL to the surface of the TGs containing lipid droplets (LD) (64-66). Previous studies shown that *in vivo* function of ATGL are determined not only by its lipase activity, but also by its LD localization and the interaction with a co-activator CGI-58 (67, 68).

Two important proteins regulate ATGL activity, 1. Comparative gene identification-58 (CGI-58) stimulates the activity of ATGL (69, 70), 2. G0S2 inhibits ATGL activity (25,71). Both of these proteins mediate their activity by binding to minimal patatin C-terminal domain (68, 72). Moreover ATGL was shown to directly interact with pigment epithelium derived factor (PEDF) in liver (73, 74). PEDF positively regulates ATGL mediated lipolysis, which was seen in PEDF deficient hepatocytes exhibiting increased TG accumulation in liver (73).

The important negative regulator of ATGL is G0S2. Hence G0S2 specifically interacts with ATGL through the hydrophobic domain of G0S2 and patatin domain of ATGL and attenuates ATGL triglyceride hydrolase activity (70). Liu et al studied the triglyceride hydrolysis *in vitro* when ATGL is incubated with G0S2 and CGI-58. CGI-58 stimulated triglyceride hydrolysis whereas the addition of G0S2 reduces the

co-activation of ATGL by CGI-58 (25). Moreover the addition of recombinant G0S2 to extracts of brown and white adipose tissue inhibited lipolysis in a dose dependent manner (53).

Similarly, the knockdown of endogenous G0S2 accelerates basal and stimulated lipolysis in adipose tissue, whereas over-expression of G0S2 reduces the rate of lipolysis in both adipose tissue explants and adipocytes (25). Liu et al demonstrated that G0S2 is recruited to lipid droplets only by direct interaction with ATGL; the knockdown of ATGL eliminates G0S2 localization to lipid droplets and both G0S2 and ATGL translocates to lipid droplet following the activation of β- adrenergic receptor (71). Moreover, the mice lacking ATGL die prematurely due to triglyceride deposition in multiple tissues (53, 75). In addition, over-expression or silencing of G0S2 in SGBS adipocytes decreases and increases lipolysis, respectively (76) and G0S2 also regulates human lipolysis by affecting enzyme activity and intracellular localization of ATGL (76). Increased lipolysis contributes to insulin resistance and development of type 2 diabetes. Reduced G0s2 mRNA and protein levels were seen in poorly controlled type 2 diabetic patients supporting the role of G0S2 in regulating lipolysis and prognosis of diabetes (77, 78).

Following the 24h fasting both ATGL mRNA and protein levels are increased whereas fasting reduces both *G0s2* mRNA and protein levels in adipose tissue but increases in liver (24). These changes lead to an increase in lipolysis (24, 78, 79). Yang et al showed that tumor necrosis factor-α (TNF-α) stimulates basal lipolysis in adipocytes by decreasing the level of G0s2 mRNA and co-expression of G0S2 significantly decrease TNF-α induced lipolysis (80). These findings suggested that early reduction of G0S2 content permits TNF-α induced lipolysis. In addition, adipocyte specific over-expression of

G0S2 led to significantly decrease basal lipolysis in mesenteric adipose tissue of chow fed mice (78, 81).

Thus, G0S2 acts as a negative regulator of ATGL and TG hydrolysis both in cell culture and *in vivo* (82, 25). The mechanism by which G0S2 inhibits lipolysis is not completely understood. It was suggested that G0S2 may compete with CGI-58 for access to ATGL and thus inhibits the activation of ATGL by CGI-58 (25). Recently it was shown that the expression of G0S2 increases during the cell cycle entry suggesting that lipolysis may be regulated during the cell cycle (25).

Instead, mice that over-express ATGL have increased lipolysis and are protected from diet induced obesity (83, 84, 52). Previous studies have shown that mice lacking ATGL die prematurely due to triglyceride deposition in multiple tissues (53). Mutations in human ATGL and CGI-58 were identified as a cause for various neutral lipid storage diseases and ichthyosis (85). Another study has shown that ATGL is also involved in lipid droplet degradation in nonadipocyte cells (86, 87). Both ATGL and CGI-58 mutations produce hepatomegaly and liver steatosis (86, 88-91).

1.7. Regulation of Lipolysis by G0S2

Figure 1.2 shows the regulation of lipolysis by G0S2 under basal and stimulated conditions. To summarize the figure, triglycerides are synthesized during feeding. Adipocyte reduces lipolysis to maximize triglyceride packaging into lipid droplets. The protein perilipin coats lipid droplet and, under fed conditions, limits lipase access to neutral lipid substrates, thus reducing lipolysis. Perilipin forms a complex with CGI-58 making unavailability of CGI-58 for ATGL activation whereas G0S2 directly binds to ATGL and inhibits its activity. During fasting and while exercising, several signaling cascades trigger lipolysis. In the best characterized pathway, catecholamines bind

to β-adrenergic receptors on the plasma membranes of adipocytes, initiating a G protein-mediated signaling cascade, which elevates cAMP levels and activates protein kinase A (PKA). Phosphorylation of perilipin A (83) and CGI-58 by PKA promotes dissociation of perilipin from CGI-58. Now the CGI-58 competes with G0S2 to ATGL and activates TG lipolysis. Perilipin activates hormone sensitive lipase and triggers lipolysis (87). In addition, phosphorylation of carboxy-terminal serine residues of perilipin is required to

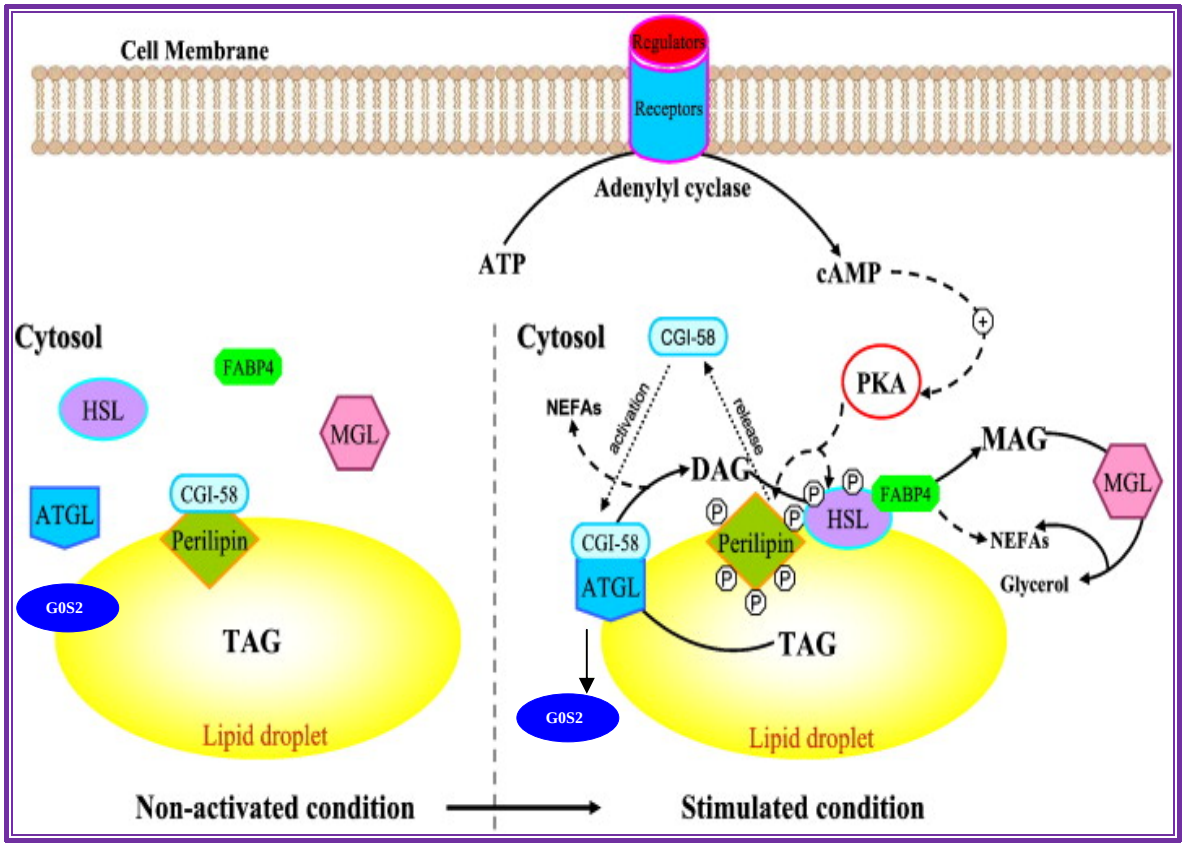

Figure 1.2: Protein localization during triglyceride storing and lipolytic conditions. Under fed conditions, triglycerides are packaged into perilipin-coated lipid droplets. Both ATGL and hormone-sensitive lipase are sequestered in a non-lipid droplet compartment; ATGL is bound to G0S2 whereas perilipin forms a compex with CGI-58 on the surface of lipid droplets. Under starvation and exercise, β-adrenergic receptor is activated which activates protein kinase A signaling cascade leading to the phosphorylation of CGI-58, perilipin and hormone sensitive lipase. Phosphorylation of perilipin causes dispersion of CGI-58 and now the CGI-58 competes with G0S2 for ATGL and activates hydrolase activity. Whereas perilipin A activates hormone sensitive lipase to facilitate the hydrolysis of diacyglycerol. Monoglyceride lipase hydrolyses monoglyceride into glycerol and free fatty acid. The released free fatty acids and glycerol are exported from the adipocyte to fuel energy production in skeletal muscle and other tissues (87).

facilitate triglyceride hydrolysis by ATGL through an as yet unknown mechanism.

1.8. G0S2, Regulator of Cell Cycle

The G0/G1 switch gene 2 (*G0s2*) was initially identified and shown to be expressed in lectin stimulated mononuclear cells and it is necessary for resting cells to enter G0 to G1 phase of the cell cycle (18). The cell cycle regulatory function of G0S2 is further supported by the reduced proliferation of cardiac fibroblast showing increased expression of cell cycle inhibitor G0S2 (20). Conversely, the very low expression of G0S2 in proliferating hepatoma cell lines in comparison with growth arrested mouse liver suggest that the role of G0S2 in growth arrest and differentiation. These results suggest that G0S2 has cell type specific function; but the reason for this discrepancy is not clear (21). Additionaly, gene expression analysis in proliferating preadipocytes showed that down regulates mRNA levels of C/EBPα and up regulates mRNA levels of G0S2 in monocytes (92). These data indicate that circulating peripheral blood monocytes can disrupt adipogenesis by interfering with a critical step in C/EBPα and G0S2 transcription required for preadipocytes to make the transition from proliferation to differentiation (92).

Recently it was shown that G0S2 is regulated in aged human dermal fibroblasts suggesting that G0S2 may have a role in skin aging (93). Moreover, elevated level of G0S2 correlate with low frequency of CD34-positive cells in the peripheral blood and low counts of colony-forming cells in vasculitis, psoriasis and rheumatoid arthritis (94-96).Yamada et al showed that G0S2 maintains quiescence in hematopoietic stem cells by sequestration of nucleolin in the cytosol (16, 97).

1.9. Liver Regeneration

The accumulation of fat during liver regeneration was shown to be essential for efficient hepatocellular proliferation (98). In line with this, mice that are

deficient in Caveolin-1 have reduced lipid droplet accumulation and reduced survival during liver regeneration (99). These studies raised the possibility that transient liver steatosis is necessary for liver regeneration after partial hepatectomy (100, 101) On the other hand, excessive fat accumulation in liver was shown to impair liver regeneration (102) but mice with altered hepatic triglyceride content failed to show an effect on liver regeneration (103). Thus, the delineation between beneficial and detrimental deposition of fat during liver regeneration is still under debate. Mice that undergo starvation have impaired liver regeneration (104, 105) and the mechanism of this phenomenon was thought to be the transient fat accumulation in liver observed during starvation. However, up to date no further studies addressed molecular factors involved in this phenomenon.

1.10 AIMS

G0s2 represents one of the subfamily of G0s genes. Studies on *G0s2* indicate that the gene may have a role in both cellular proliferation and regulating the apoptosis. In addition, G0S2 regulates lipolysis by inhibiting adipose triglyceride lipase (ATGL). These processes could be relevant for the maintenance of tissue and organ homeostasis and also for providing free energy for cellular metabolism. However, *in vivo* studies on the functional role of G0S2 have not been conducted in mouse models to address this question. The main aim of my doctoral studies was to analyze consequences of *G0s2* deletion in a knockout mouse to delineate its role in cellular proliferation, apoptosis and regulation in the fat metabolism.

2. Materials and Methods

2.1 Laboratory equipment

Cell Culture Incubator	Sanyo
Cell Culture Laminar Flow Bench	Biowizard
Cell viability analyzer Vi-Cell XR Coulter	Beckman
Avanti Centrifuge Coulter	Beckman
Allegra Centrifuge Coulter	Beckman
Chemiluminescence	Vilber Lourmat
Cryotome	Microm
FACS Calibur	BD Biosciences
LSR II	BD Biosciences
FACSAriaTM II	BD Biosciences
PCR Cycler	SensoQuest
7300 Real Time PCR System Biosystems	Applied
Animal Blood Counter	VetABC
Microscope	Leica
Ultracentrifuge Coulter	Beckman
Thermomixer	HLC
Fluorescent Image Analyzer FLA-3000	Fujifilm

2.2 Software

Leica LAS AF Leica Microsystems	Leica
Flowjo 7.2.2	Tree Star
GraphPad Prism 5	GraphPad Software
TFL-Telo V2.2.07.0418	Provided by Peter Lansdorp
BASReader 3.14	Raytest
Aida Image Analyzer V.3.12	Raytest

2.3 Chemicals and Biochemicals

Chemical	Supplier
Acrylamide	Roth
Agarose	Sigma
Ammonium chloride	Roth
Ammonium per sulphate	Merck
Bromophenol blue	Serva
BSA (Bovine Serum Albumin)	PAA
Bradfords Dye	BioRad
Chloroform	Merck
Chemiluminescent HRP substrate	Millipore
Diethylpyrocarbonate (DEPC)	Sigma
Dimethyl sulfoxide	Sigma
Dithiothrietol	Sigma
dNTPs	Bioline
Disodium hydrogen phosphate	Merck
DAPI	Vectashield
EDTA (N, N; N', N' – Ethylenediaminotetracetic acid)	Calbiochem
ENU (N-ethyl-N-nitrosourea)	Sigma
Ethanol	Sigma
Ethidium bromide	Merck

2.4 Animal work

2.4.1 Generation of *G0s2* Straight Knockout Mouse

The Cre-loxP system has been used for genetic modification of specific genes in germ lines and specific organs. Two LoxP (or FRT) sites can be inserted into two introns of target gene by homologous recombination and flanked target gene can be excised by the expression of site specific DNA recombinase Cre (or Flip, FLP) in mice. Using germ line Cre transgenic mice, a flanked gene can be deleted in the germ line or in specific tissue. In this study, we used the Cre- deleter transgenic mouse line to delete the *G0s2* in the germ line tissue (106).

A conditional gene targeting vector was designed and constructed by Dr. Luis M. Guachalla. Institute of Molecular Medicine, Ulm University. Two loxP sites were inserted into two introns to flank exon 2 (Fig 2.1), which has two FRT sites flanking a neomycin resistant selection cassette, aminoglycoside phosphotransferase, in intron 2. Electroporation of targeting vector into ES cells and blastocyst injection were performed with collaboration of Dr. Raija Soininen, Institute of Biomedicine, and University of Oulu, Finland. Southern blot analysis to screen and verify ES cell cones was performed by a collaborator Dr. Luis M., Institute of Molecular Medicine, Max -Planck research group on stem cell ageing, Ulm University.

ES cells used for gene targeting were derived from C57BL/6J mice and injected into the cavity of a blastocyst. Chimeric offsprings were mated with C57BL/6J mice and germ-line transmission of the floxed allele was determined by southern blot analysis of genomic DNA from tails of newborns. Heterozygous F1 mice were crossed with a embryonic Cre-deleter transgenic line under CMV-promoter, Cre lines were on a C57BL/6J background.

2.4.2 Primers For Genotyping and RT-PCR

Genotyping of the mice was performed using a PCR based method.

Chromosomal DNA from mouse tails and the following primers were used in this method:

G0s2FP **- 5'-** agcaagtgctgcctctcttc **-3'**

G0s2RP **- 5'-** gtctcaactaggccgagcac **-3'**

G0s2 delRP - 5' – cttgaatactgcctggcaca **-3'**

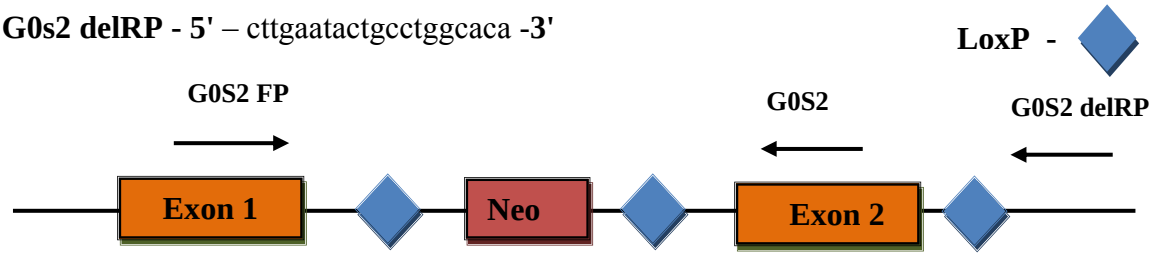

Figure 2.1 Genotyping strategy and location of primers.

The primers (G0s2 FP, G0s2 RP and G0s2 delRP) were used to genotype wild type and deleted allele. The wild type allele gives a 400bp and for the deleted allele 200bp (Fig.3.2).

2.4.3 Maintenance and Handling of Animals

Animals were bred and maintained at the central animal facility of the University of Ulm. All animal handling was done according to the guidelines of the animal facility committee. All animal experiments were accepted by the Regierungspräsidium of Baden-Würtemberg. The mice were housed in a day-night rhythm of 12h and were fed and watered *ad libitum*. The mice were fed on 30% high fat diet for the induction of obesity and diabetes. The high fat diets are purchased from the company ssniff, Germany. The overnight starvation experiments were done in the central animal facility.

2.5 Immunohistochemistry:

2.5.1 Processing of Tissues

Mice were sacrificed via CO_2 asphyxiation, organs were quickly removed and

either frozen down on dry ice or fixed in 4% buffered paraformaldehyde (PFA) for paraffin embedding. Blood counts were analyzed by a Vet ABC machine. The plasma was collected and frozen down after centrifugation at 2800rpm, 5min, and 4°C for later analysis.

2.5.2 Immunohistochemistry Staining For Tissues

The 5µm paraffin sections were dewaxed by passing through xylol and rehydrated by incubation in a series of graded ethanol dilutions 100%, 90% and 70% for 5min each. Epitope retrieval was performed by preheating the sections 5min at full power (microwave, 900W) in 10mM sodium citrate buffer pH 6.5 until boiling, followed by 10min at a sub-boiling temperature (600W). The sections were washed in PBS and stained with primary antibody (Oncogene Science, Uniondale, NY; diluted 1:150 in phosphate-buffered saline in PBS, overnight at 4ºC. This was followed by washing in Tris Borate Saline –Tween (TBS-T) and subsequent incubation for 1h with secondary anti-rabbit IgG conjugated with Cy3. Lastly the slides were washed and mounted with mounting medium including DAPI. The slides were stored at 4°C until further analysis.

2.6 Protein analysis

2.6.1 Protein Isolation and Concentration Measurement:

Whole cell lysate was prepared using RIPA buffer (1% Nonidet P-40, 0.5% Sodium Deoxycholate, 0.1% SDS, 150mM NaCl, 50mM Tris-HCl (pH 8.0), 50mM DTT, 1mM sodium metavanadate, 1mM PMSF, and 10% protease inhibitor cocktail (Roche, 11836153001). Tissue samples were homogenised and rotated at 4ºC for 30min followed by centrifugation at 13,000rpm for 15min. The supernatant was collected and stored at -20ºC until further use. Total protein concentration was estimated by performing the Bradford assay (Biorad protein assay Cat # 500-0006), using a standard curve of known

BSA concentration.

2.6.2 Western Blotting

Protein samples were denatured using 4x SDS Laemmli buffer at 95ºC for 10min and then separated in a 10-15% polyacrylamide gel electrophoresis along with protein molecular weight marker (Biorad Cat 61-0373). After electrophoresis, protein was transferred on to a PVDF membrane (Millipore IPVH00010) using BioRad semi dry western transfer apparatus. The membrane was blocked with 5% skimmed milk powder (Roth, Germany) in TBS containing 0.1% Tween 20 (TBS-T) for 1h at room temperature. The membrane was incubated overnight with primary antibody diluted in 5% skimmed milk powder in TBS-T at 4ºC. Post incubation the membrane was washed for 15min for 4 times with TBS-T and incubated with HRP conjugated secondary antibody for 1h at RT, followed by five TBS-T washes of 15min each. The blot was developed using chemiluminescent HRP substrate (Millipore) and luminescence was measured with a luminescence documentation system (Vilber Lourmat). Each individual experiment was repeated 2-3 times.

2.7 RNA Analysis:

2.7.1 RNA Isolation

Total RNA was isolated using the TRIzol LS reagent (Invitrogen, 10296-010) or RNeasy Mini Kit (Qiagen, 74104; according to the manufactures protocol). Frozen tissues were ground to powder on dry ice immersed in liquid nitrogen using mortar and pestle. 750µl of TRIzol was added to pulverized tissue (or fresh cells), volume was adjusted to 1ml with DEPC-treated water and vortex mixed for 15sec. Samples were incubated for 5min at room temperature, invert mixed for 6 times with additional 200µl of chloroform, and incubated for 5min at room temperature. The phase separation was

performed by centrifugation at 4°C, 12,000rpm for 5min. The colourless upper aqueous phase was collected and equal amount of isopropanol was added, followed by 10min incubation at room temperature. The suspension was centrifuged at 12,000rpm for 30min, 4°C to precipitate the RNA. The RNA pellet was washed twice with 75% ethanol and dissolved in DEPC treated water. RNA concentration was measured with a nanophotometer or Bio analyzer, a 260/280 and 230/260 ratio of more than 1.8 absorbance units was considered a good RNA preparation.

2.7.2 DNase I Treatment

Extracted RNA was treated with DNase I (Roche, 04716728001) to avoid residual genomic DNA contamination. 0.5U DNase I was added per µg of RNA, followed by incubation at 37°C for 15min. The reaction was terminated by adding 8mM EDTA (pH 8.0) and heating at 75°C for 10min.

2.7.3 cDNA Synthesis

cDNA synthesis was performed using Superscript™ III first-strand synthesis Kit (Invitrogen, 18080-051) according to manufactures protocol. Briefly, the reaction mixture containing 0.5-1µg of DNase treated RNA and SuperScript™ III/ RNaseOUT™ enzyme was incubated at 25°C for 10min. The RT reaction was carried out at 50°C for 30min, followed by a termination step at 85°C for 5min. After cDNA synthesis, RNA was digested by 1 unit of RNase H (Invitrogen, 18021-014) at 37°C for 20min and stored at -80°C until further use.

2.7.4 Quantitative Real Time PCR and Microarray

Relative gene expression analysis was done with the help of quantitative real time PCR method using TaqMan probes. 500ng of cDNA was used per assay reaction. Gene expression was measured relative to GAPDH or 18s rRNA as an internal control.

Each individual sample was measured in triplicates and all the experiments were repeated 2-3 times. For microarray analysis, total RNA was isolated using the RNeasy Mini Kit (Qiagen, Valencia, CA) according to the manufacturer's instructions. The quality of the RNA was analyzed with the 2100 Bioanalyzer (Agilent Technologies, Santa Clara, CA). Samples with a RIN factor more than 6 were used for further analysis.

2.8 Fat Measurement

2.8.1 *In vitro* Adipogenesis Assay

MEF's were isolated from E12.5 embryos according to standard protocols. Briefly, after removal of the head and liver, tissue was rinsed twice in ice-cold PBS and minced in trypsin/EDTA (Gentaur, L 2153) on ice using either scissors or a scalpel blade. After 15-30min of incubation at 37°C, cells were resuspended in medium, and plated in 10-cm plates. Primary MEF's were grown in DMEM (Sigma, D6429) containing 10% fetal bovine serum, 100U/ml penicillin, 0.1µg/ml streptomycin. Two days after the MEF's are grown to confluent treat MEF's with - IBMX (Iso butyl methyl xanthine), dexamethasone, insulin and troglitazone (PPAR gamma agonist). Replenish the media with insulin and troglitazone for every 2 days and on day 13, cells were fixed and stained with Oil Red O according to the standard protocol. The Oil Red O stained fat are eluted by adding 100% isopropanol and measured the OD at 500nm.

2.8.2 High Fat Diet

The 30% high fat diet food (ssniff® EF R/M with 30% Fett, 10mm pellets Cat no. E15126-34) are purchased from ssniff company from Germany.

2.8.3 Fat Staining and Triglyceride Quantification

For the fat staining, 5µm thick liver cryosections were fixed in 10% formalin

for 7min. The liver sections were dried for 60min at room temperature and placed in absolute propylene glycol for 5min. Then, sections were stained with freshly prepared pre-warmed Oil Red O (Sigma, O0625) solution at 65°C for 10min. After rinsing in 85% propylene glycol solution for 5min and the slides were washed for twice in water for 5min. The sections were lightly stained with haematoxylin and rinsed twice in water for 5min.

The triglyceride quantification in liver was done with triglyceride assay kit form Bio-vision (Cat. # K622-100). 100mg of liver tissue is homogenized in 1ml solution containing 5% NP-40 in water. Slowly heat the samples to 80-100^{0}C in a water bath for 5min or until the NP-40 solution becomes cloudy, then cool down to room temperature. Centrifuge at high speed for 2min to remove any insoluble material. The triglycerides present in NP-40 is mixed with lipase and triglyceride probe. The amount of triglyceride present in liver tissue is measured at 570nm.

2.8.4 Assay for Triglyceride Hydrolase Activity

Different amounts of recombinant protein lysates (10–200mg) were incubated in a final volume of 100ml buffer A with 100ml of substrate in water bath for 60min at 37°C. Substrate was prepared by emulsifying 0.33mM triolein (Sigma, St. Louis, USA), 0.45 mM phosphatidylcholine/ phosphatidylinositol (3:1, Sigma, St. Louis, USA), 0.5% defatted BSA (Carl Roth GmbH, Karlsruhe, Germany) and ^{3}H triolein (10,000 cpm/ml; Perkin Elmer Life Sciences, Waltham, USA) as a radioactive tracer as described. In control experiments, lysates of cells expressing only the N-terminal tags (Gb1, smt or Trigger factor -TF) were used. Reactions were terminated by addition of 3.25ml of chloroform/heptane/methanol (9:7:10) and 1ml of 0.1M potassium carbonate, 0.1M boric acid pH 10.5 and fatty acids extracted by vortexing. After centrifugation (8006g, 15min), radioactivity in 1 ml of the upper phase was determined by liquid scintillation counting.

Activation of ATGL was achieved by addition of purified CGI-58 (2.5mg/100ml reaction). Inhibition of ATGL in the presence of CGI-58 was tested by adding bacterial lysate containing G0S2.

2.8.5 Growth Curve

MEF's were isolated from E12.5 embryos according to standard protocols. Primary MEF's were grown in DMEM (Sigma, D6429) containing 10% fetal bovine serum, 100U/ml penicillin, 0.1µg/ml streptomycin. Growth was monitored over a period of 25 days and population doublings were calculated.

2.8.6 Partial Hepatectomy (PH)

Partial hepatectomy (PH) was conducted in 2-3 month old mice fed ad libitum (complete access for food) or fasted for 20h previous the operation. Mice had free access to food and water after PH and were sacrificed at the respective time points.

All mice were operated in the morning (between 9 to 11 a.m.). Mice were anesthetized and subjected to a standard two-third partial hepatectomy by surgically removing the left lateral, left median and right median lobes. The mice were sacrificed at 0h, 38h and 48h after partial hepatectomy to analyse liver regeneration.

2.9 Southern Blot Analysis

2.9.1 Genomic DNA Isolation from Tissue

Genomic DNA was isolated using the conventional Phenol/Chloroform method from minced tissues or cultured cells. An equal volume of phenol was added to cell lysate, followed by treatment with a mixture of phenol: chloroform: isoamyl alcohol (25:24:1) to get rid of additional contaminating proteins. DNA was precipitated with a equal volume of isopropanol and 0.5M NaCl, washed with 70% ethanol. Genomic DNA

was resuspended in either TE buffer [10mM Tris-Cl (pH 7.5), 1mM EDTA] or autoclaved water and kept in a shaker at 37°C for 2-3h. To prevent DNA degradation, DNA was not incubated for more than 3h.

2.9.2 Southern Blot Analysis of *G0s2*

20μg of genomic DNA was digested with either 80U of *Stu*I overnight at 37°C. Digested genomic DNA was loaded onto a 0.8% agarose gel in 0.5xTAE (45mM Tris-acetate, 1mM EDTA) and run at a low voltage (40-60V) overnight. Gel was then photographed with a ruler to later identify band position and pre-treated by soaking in a series of solutions for depurination (0.25M HCl, 20min), denaturation (1.5M NaCl/0.5M NaOH, 30min), and neutralization (1.5M NaCl, 0.5M Tris-HCl, pH 7.0) of the DNA and gel matrix. The DNA was blotted onto a nylon membrane, Hybond-N+ (GE healthcare, RPN303B) via upward capillary transfer for 16h. The membrane was then washed in 50mM NaPi (1M NaPi: 0.5M Na_2HPO_4, pH 7.2) solution for 10min, air dried and followed by DNA fixation using 120mJ/cm^2 UV cross-linking.

Pre-hybridization and hybridization were performed at 65°C with Church's buffer (0.5M NaPi, 7% SDS, 1mM EDTA, pH 8.0). PCR products (Probe A, B) were labelled with [α-^{32}P] dCTP using Rediprime II DNA labelling Kit (GE healthcare, RPN 1633). To remove unincorporated ^{32}P-labeled nucleotides, the reaction mixture was subjected to gel filtration using illustra microspin G-50 columns (GE healthcare, 27-5330-01), and the activity was measured by a liquid scintillation analyzer (PerkinElmer, Tri-Carb 2810TR). Heat denatured ^{32}P-labeled probe was added to hybridization solution at 1x10^6 cpm/ml and hybridized for overnight. Membrane was washed in following SSC dilution series (all solutions contain 0.1% SDS), 2x SSC, 5min, RT; 1x SSC, 15min, RT; 1x SSC,15 min, 65°C; 0.5x SSC,15min, 65°C; 0.1x SSC, 15min, 65°C). The hybridized

bands were then detected by phosphoimager (Fujifilm, FLA-3000) and the band positions and intensities were analysed by Aida Image Analyzer (Raytest, V.3.12).

2.10 FACS Analysis

2.10.1 Bone marrow

Bone marrow analysis was performed in freshly isolated cells that were flushed out with PBS from tibias, femurs, and spine of the sacrificed mice. Red blood cell lysis was performed for one minute in 1ml of lysis solution (150mM NH_4Cl, 10mM $KHCO_3$, EDTA pH 8 0.1mM) and neutralized with PBS. Cells were counted and adjusted to the cell density required for the experiments with ice- cold staining media (PBS with 2% FBS and 0.02% sodium azide).

Table 1: Surface marker combination for the identification of haematopoietic lineages

Staining	FITC	PE	PerCP -Cy5.5	PE-Cy7	APC	APC-Cy7	Cell number
B & T Cells		B220	CD4 CD8	Gr-1	CD11c	CD11b	2 x 10^6
HSC	Annexin V	Flt3	IL7R	Sca1	cKit	Lin-Bio* SA**	2 x 10^6
Myeloid Progenitor	FcgR	Flt3	IL7R	Sca1	cKit	Lin-Bio* SA**	2 x 10^6
Cell Proliferation	Ki67						5 x 10^6

*Lin-Bio: biotinylated lineage negative cocktail (Anti-Gr1, Ter119, B220, CD11b, CD3, CD4,CD8)

**SA : streptavidin conjugated-APC-Cy7

Bone marrow cells were stained using the indicated antibodies for the following staining:

The cells were stained in 10-50µl of staining medium for 30min in a dark chamber at 4°C. Cells were then washed with 1ml staining medium at 2800rpm for 5min at 4°C. For

HSC staining, cells were stained with biotinylated anti-lineage antibody cocktail for 30min, washed, and then stained with the secondary streptavidin conjugated antibody for another 1h (for CD34 staining). After washing, cells were resuspended in 300-500ul staining media and filtered with a nylon net filter, pore size 60µM (Millipore, NY6000010) for FACS analysis. Similarly, for checking the proliferation cells were stained with anti Ki67- Alexa 488 antibody in addition to DAPI. All analysis was performed on BD LSR II and using the FlowJo 887 software.

3. Results

3.1. Generation of *G0S2* knockout mouse

Previous studies have shown that G0S2 binds to adipose triglyceride lipase (ATGL) through its C-terminal domain (71). The C-terminal domain of G0S2 is encoded by exon 2. *G0s2* gene contains two exons, which encode a protein of 103 amino acids yielding a protein of over 11kDa. The exon 1 contains kozak sequence and untranslated region (UTR) and exon 2 contains open reading frame (ORF). Dr.Luis Guachalla in our group generated conditional *G0s2* knockout mice carrying two loxP sites flanking exons 2 (encoding the C-terminal aa 1-103, which mediates ATGL binding) and consisting of a 4Kb long arm followed by a loxP site and a 2Kb short arm that followed the neo cassette

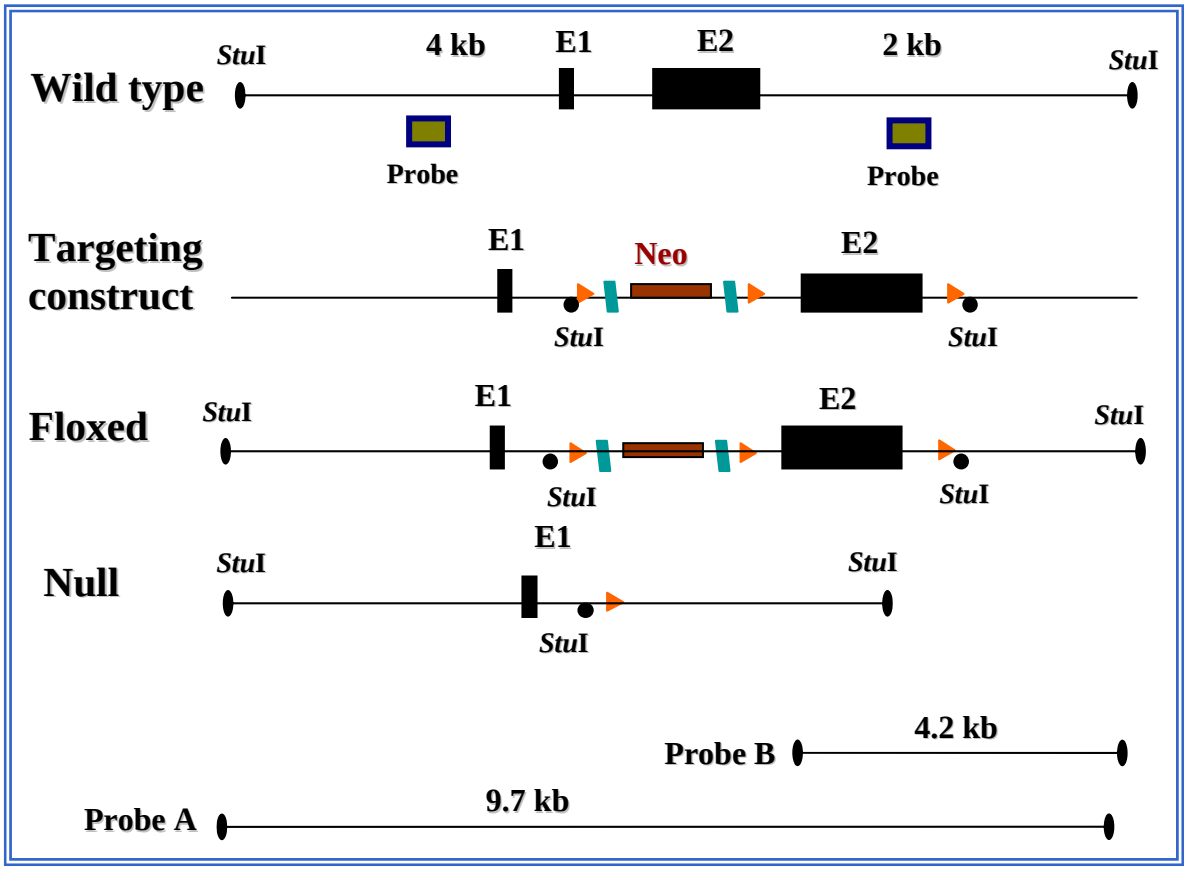

Figure 3.1: Targeting strategy for loxP-flanked *G0s2* conditional knockout mice. Schematic of the mouse *G0s2* locus on chromosome 1 (NCBI Gene ID: 14373), the targeting construct, neomycin resistant cassette, deleted floxed allele, and the altered allele of *G0s2*. Probe A, B: southern probes, red bar: loxP sites, orange triangles: frt sites, gray bar: neomycin resistant cassette, red bar.

and a third loxP site after exon 2 (Fig.3.1). To test whether a germline deletion of *G0s2* was viable, the mice were crossed with a germline deleter mouse carrying a Cre-expression cassette under the CMV promoter.

The targeting vector was designed and constructed by Dr. Luis Guachalla and electroporation of targeting vector was performed by Dr. Raija Soininen (as described in 2.4.1). To verify embryonic stem (ES) cell clones containing flanked exon 2 in the *G0s2* gene locus, genomic DNA isolated from more than 400 ES cell clones was further analysed by southern blot.

DNA was digested with *Stu*I and subjected to southern blot analysis using two external probes, Probe A (left arm) and Probe B (right arm), to detect homologous recombination of *G0s2* locus. The targeted ES clone A21 shows the two expected band sizes of the wild type allele (9.7Kb) and targeted allele (4.2 Kb) by using either probe A or probe B (Fig.3.2A). The ES clone A21 was then injected into the blastocysts and the chimeric mice were born. ES cells were derived from an C57BL/6J strain. Chimeras were crossed with C57BL/6J mice to obtain germ line transmission.

To verify germ line transmission, PCR based genotyping was performed using the primers g0s2FP/g0s2RP/g0s2gLxF1 to amplify a 382bp wild type band and a 242bp targeted band. Since *G0s2* targeted allele contains a neomycin resistant cassette flanked by FRT sites; mice were crossed with FLP deleter mouse line, flippase transgenic mouse, to remove the FRT-flanked neo cassette. The mice received were next used to delete *G0s2* gene through crossing them with a germline deleter mouse carrying a Cre-expression cassette under the CMV promoter (112).

To achieve germ line deletion of *G0s2*, heterozygous floxed mice ($g0s2^{fl/+}$) were crossed with Cre-Del^{+} transgenic mice which lead to $g0s2^{+/-}$ lacking exon 2 in one

allele of *G0s2* gene in the mouse embryo. From the inter-cross matings of heterozygous *g0s2*$^{+/-}$ mice, homozygous *g0s2*$^{-/-}$ mice were obtained in the expected mendelian ratio indicating that *G0s2* is dispensable for embryonic development. Genomic DNA isolated from tissues was digested with *Stu*I and subjected to southern blot using an external probe A. The 4.2Kb *g0s2* deleted band was detected in most heterozygous/homozygous tissues (Fig.3.2A). Gene deletion was also analyzed by PCR using g0s2FP/g0s2RP/g0s2delR1 primer pair, which showed a 400bp wild type band and a 200bp deleted band (Fig.3.2B). G0S2 was shown to be expressed in white adipose tissue *in vivo* and during adipogenesis

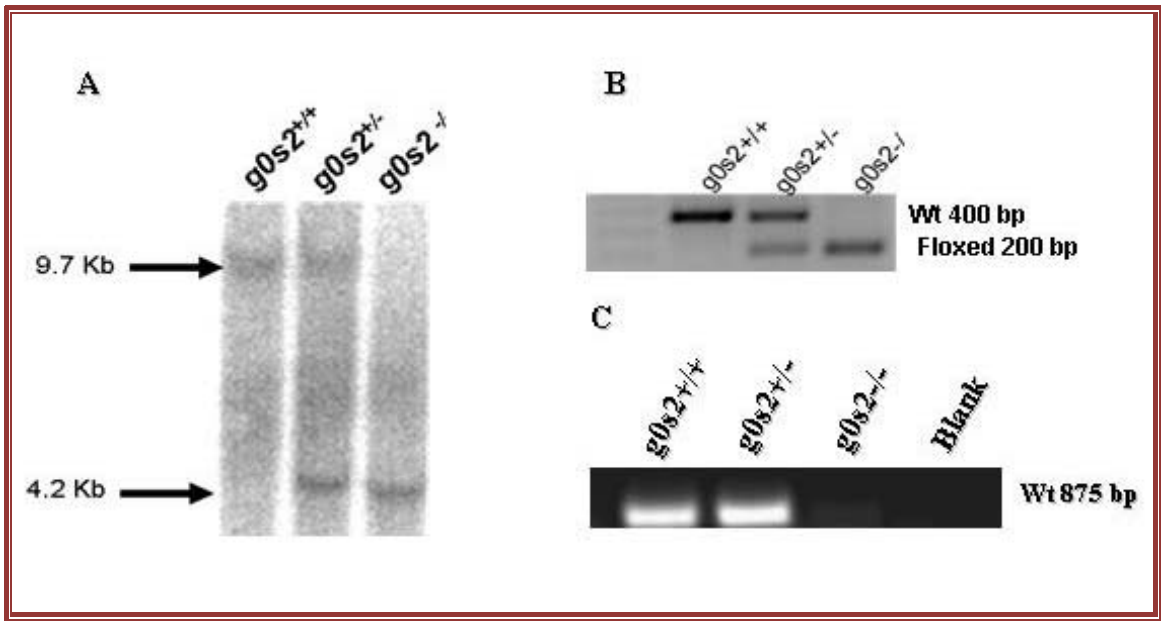

Figure 3.2. Genotyping results for *G0s2* knockout mice. A. Southern blot showing wild type *g0s2*$^{+/+}$, heterozygous *g0s2*$^{lox/-}$ and homozygous g*0s2*$^{-/-}$ mice (Probe A: WT 9.7Kb, deleted 4.2Kb; **B.** PCR results showing WT *g0s2*$^{+/+}$ (400bp), heterozygous *g0s2*$^{lox/-}$ (400bp, 200bp) and homozygous *g0s2*$^{-/-}$ (200bp) mice. **C.** RT-PCR products using exon2 specific primers against the *G0s2* transcript (875bp) in MEF's of *g0s2*$^{+/+}$, *g0s2*$^{lox/-}$ and *g0s2*$^{-/-}$ mice.

in vitro (21). RT-PCR from adipogenic induction of mouse embryonic fibroblasts (MEFs) derived from *g0s2*$^{-/-}$ mice failed to show *g0s2* mRNA expression (Fig.3.2.C).

Postnatally, *g0s2*$^{-/-}$ mice exhibited normal organ development, organ weights and blood counts of red blood cells (RBC), white blood cells (WBC) and platelets and during the observation period no overt phenotype was observed (data not shown). Male

and female *g0s2*$^{-/-}$ mice showed normal fertility.

In addition, the food intake was monitored for seven days under normal diet and there is no significant difference in the food intake between *g0s2*$^{-/-}$ mice compared to *g0s2*$^{+/+}$ mice in both male and female cohorts. The body weight and dry weight of white adipose tissue was also normal in *g0s2*$^{-/-}$ mice compared to *g0s2*$^{+/+}$ mice (Fig.3.3. A-C).

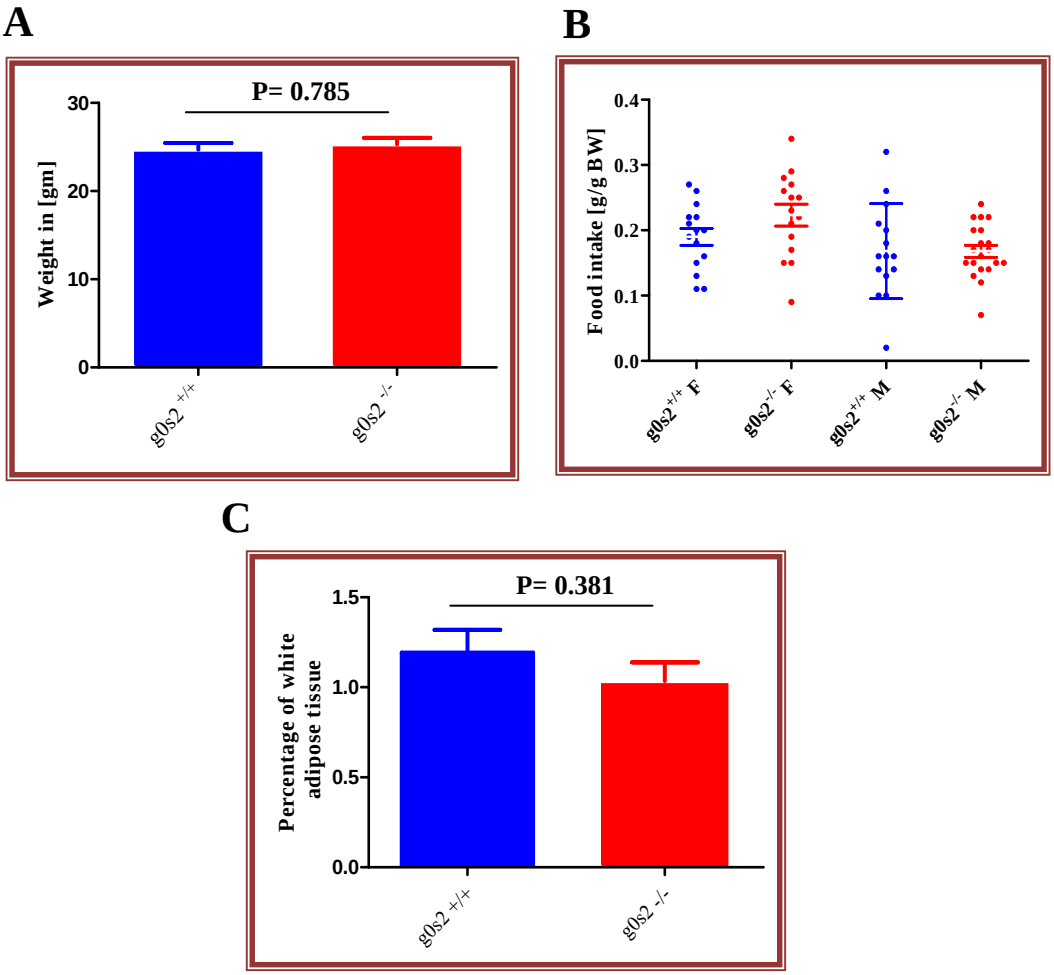

Figure 3.3: A. Bar diagrams shows the body weight of 12 weeks old wild type and knockout mice of both sex (n=8). **B.** Food intake was measured over a period of seven days in the morning (n=5 for each sex and group). **C.** The histogram depicts the percentage of white adipose tissue (WAT) normalized to body weight for mice of the indicated cohorts (n= 9 per group).

3.2. *G0s2* deletion does not induce apoptosis

A role of G0S2 in enhancing apoptosis was suggested by its unexpected interaction with Bcl-2 proteins (15). G0S2 induces apoptosis by directly interacting with

Bcl-2 and preventing its ability to heterodimerize with Bax protein (15). I evaluated the rate of apoptosis in *g0s2*$^{-/-}$ mice by exposing the mice to 9gy γ- irradiation. The ionising radiation from gamma rays induces extensive DNA damage which induces apoptosis (33) and reduces

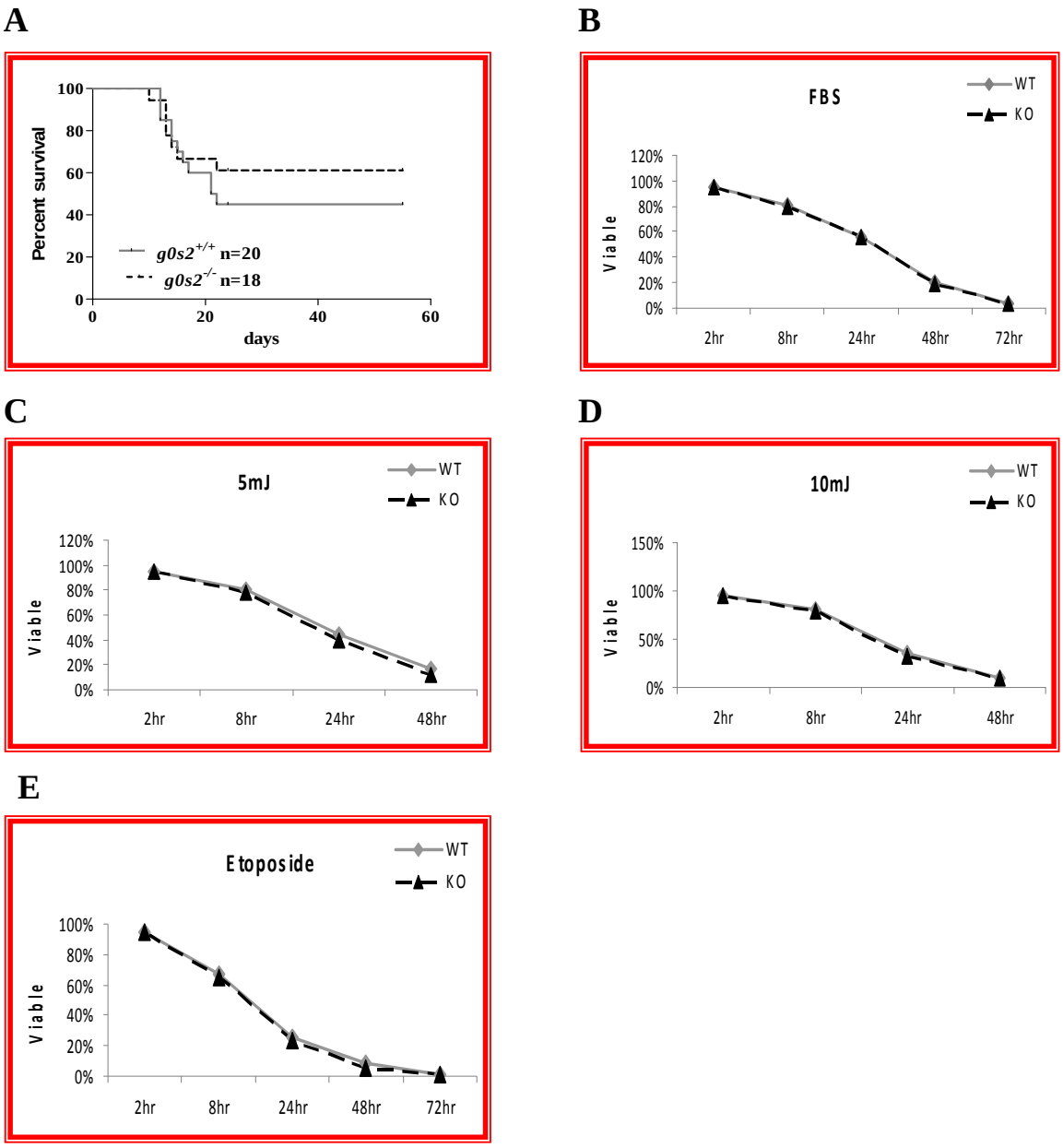

Figure 3.4: *G0s2* gene status does not affect mouse survival or the apoptosis rate in murine thymus response to gamma-irradiation or chemotherapy. A. The Kaplan Meier curve depicts the survival of 9Gy irradiated *g0s2*$^{-/-}$ mice compared *g0s2*$^{+/+}$ mice. **B-E.** The histograms depict thymocyte viability following different apoptotic stimuli.Freshly isolated thymocytes were treated with etoposide (15μM) or with 5mJ/cm^2 and 10mJ/cm^2 UV irradiation. There was no significant difference in the level of apoptosis between *g0s2*$^{-/-}$ and control groups.Abbreviations: WT- Wildtype (*g0s2*$^{+/+}$), KO- Knockout (*g0s2*$^{-/-}$).

the survival of the irradiated mice. Similarly, to evaluate the role of G0S2 in inducing apoptosis, the *g0s2*$^{-/-}$ mice were exposed to 9Gy irradiation and the survival of the mice was monitored over a period of 60 days. *G0s2*$^{-/-}$ deletion did not change the survival of the irradiated mice (Fig.3.4.A). The role of G0S2 in apoptosis was further analysed by treating freshly isolated thymocytes derived from *g0s2*$^{-/-}$ mice and *g0s2*$^{+/+}$ mice were exposed to different apoptotic stimuli such as UV and etoposide. G0S2 gene status had no significant influence on the rate of apoptosis in these experiments (Fig.3.4.B-E).

3.3 *G0s2* is dispensable for adipogenesis both in cell culture and *in vivo*

Previously reports have shown that G0S2 is up regulated during *in vitro* adipogenesis of mouse embryonic fibroblast (MEF's) and human SGBS fibroblast cell line (21). Adipogenesis was induced in growth arrested fibroblasts by IBMX (isobutyl-methylxanthine), dexamethasone, troglitazone and insulin. When fibroblasts are treated with a combination of dexamethasone, isobutylmethylxanthine, troglitazone and insulin, cells start to accumulate lipids intracellularly in the form of lipid droplets (107). Treatment of cells with dexamethasone activates the transcription factor CCAAT/enhancer-binding protein b (C/EBPb). IBMX inhibits soluble cyclic nucleotide phosphodiesterases and results in increased intracellular cAMP levels. At the nuclear level, treatment with IBMX results in activation of the related transcription factor C/EBPb and C/EBPd, that inturn induce transcription of C/EBPa and PPAR-γ (107). Within 3 days of exposure to inducers, the cells undergo differentiation. Insulin promotes adipocyte differentiation by activating PI3-kinase and Akt activity. Modulation of the activity of the fork-head transcription factor Foxo1 appears to be necessary for insulin to promote adipocyte differentiation (108). C/EBPa and troglitazone (PPAR γ-agonist) direct the final phase of adipogenesis by activating expression of adipocyte specific genes, such as fatty acid synthetase, fatty acid

binding protein, leptin and adiponectin and inhibits lipid droplet degradation (109). The adipose-specific expression of G0S2 was corroborated in mouse white 3T3-L1 four days after adipogenic induction. The maximal level of G0S2 protein expression was reached 7 days after adipogenic induction of 3T3-L1 fibroblast cells.

Given the importance of G0S2 in adipogenic differentiation, I checked the

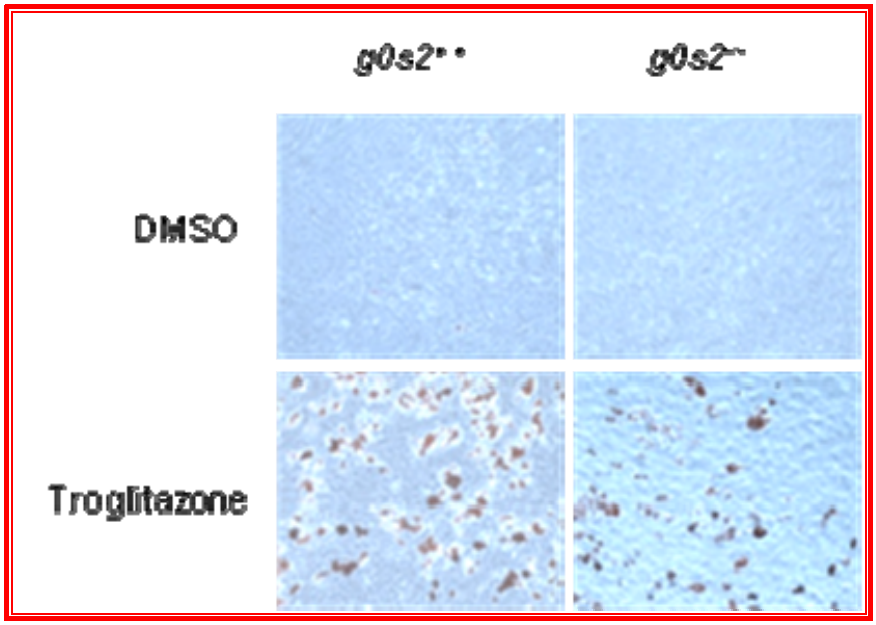

B

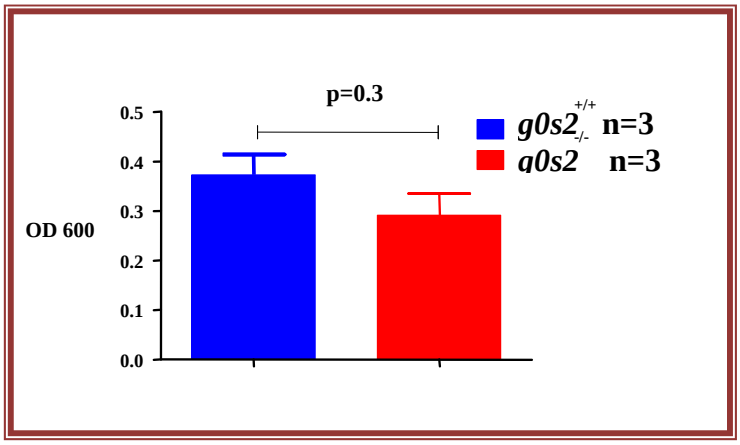

Figure 3.5: *G0s2* gene status does not affect the induction of *in vitro* adipogenesis from mouse embryonal fibroblasts (MEFs). A. Representative pictures of Oil Red O staining after adipogenic induction by using dexamethasone, isobutylmethylxanthine (IBMX) troglitazone and insulin of $g0s2^{+/+}$ and $g0s2^{-/-}$ mouse embryonic fibroblasts after 14 days of induction. **B.** Bar graphs depicting spectrophotometrical quantification (OD600) of Oil Red O after elution with isopropanol in adipogenic induced MEF's. n=3 lines per group are showed ± SEM

adipogenesis in g0s2 deleted MEF's. However, adipogenesis induction of *g0s2* deleted fibroblasts, although slightly diminished, was not significantly affected compared to *g0s2*$^{+/+}$ fibroblasts when Oil Red O deposition was spectrophotometrically quantified (Fig.3.5.A, B).

Given the role of G0S2 in inhibiting the lipolysis, g0s2 deletion was expected to accelerate lipolysis. However, in the MEF differentiation assay we could not observe a significant effect of *G0s2* gene status on adipogenesis and the build up of lipid droplets. One possible explanation was that G0S2-dependent influences on lipid metabolism were not depicted in this cell culture based system. Therefore, I wished to study the role of G0S2 in lipid metabolism in an *in vivo* system. It is known that lipolysis is enhanced during starvation. I measured the body weight of *g0s2*$^{+/+}$ and *g0s2*$^{-/-}$ mice for a period of 12 months in normal fed (ND) and high fat diet (HF) fed mice. High fat diet resulted in increased bodyweights both in males and females, but g0s2 gene status did not significantly influence body weight gain in neither normal fed diet nor high fat diet fed groups (Fig.3.6.A, B). Next, the body weight loss during 40% calorie restriction was analysed in a set of *g0s2*$^{+/+}$ and *g0s2*$^{-/-}$ mice for 25 days. Bodyweight loss and glycaemia with a 40% calorie restriction regime did not differ between *g0s2*$^{+/+}$ and *g0s2*$^{-/-}$ mice (data not shown).

3.4 *G0s2* deletion does not induce lipolysis in white adipose tissue

Given the notion that G0S2 regulates lipolysis by inhibiting adipose triglyceride lipase (ATGL), I measured the activity of ATGL in white adipose tissues. Freshly isolated white adipose tissues was placed in high glucose DMEM containing 0.5% defatted bovine serum albumin medium. CGI-58 was added to activate lipases (ATGL and hormone sensitive lipase (HSL), to determine the activation of ATGL, an HSL inhibitor

A

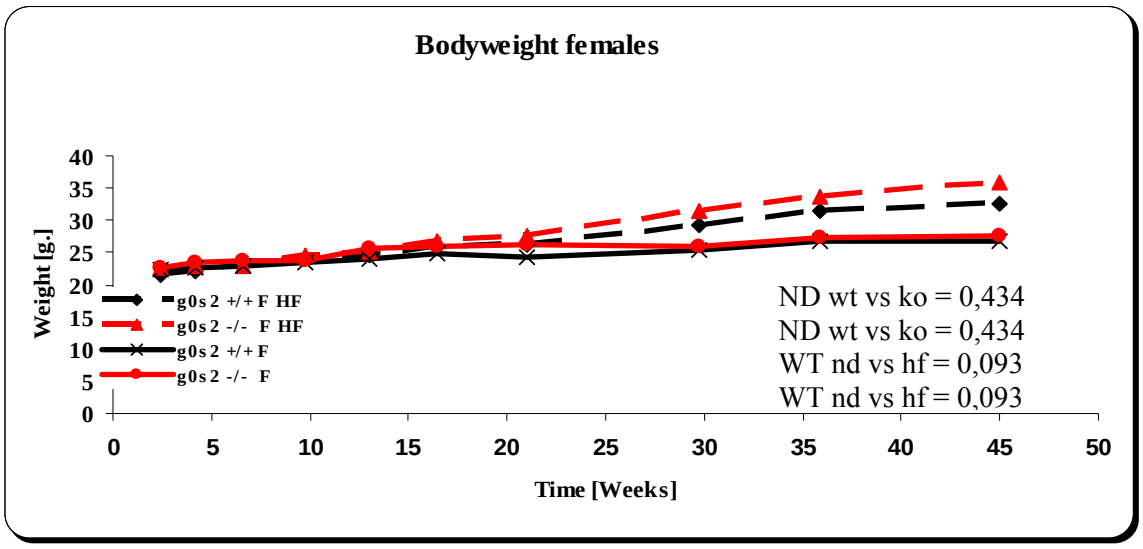

B

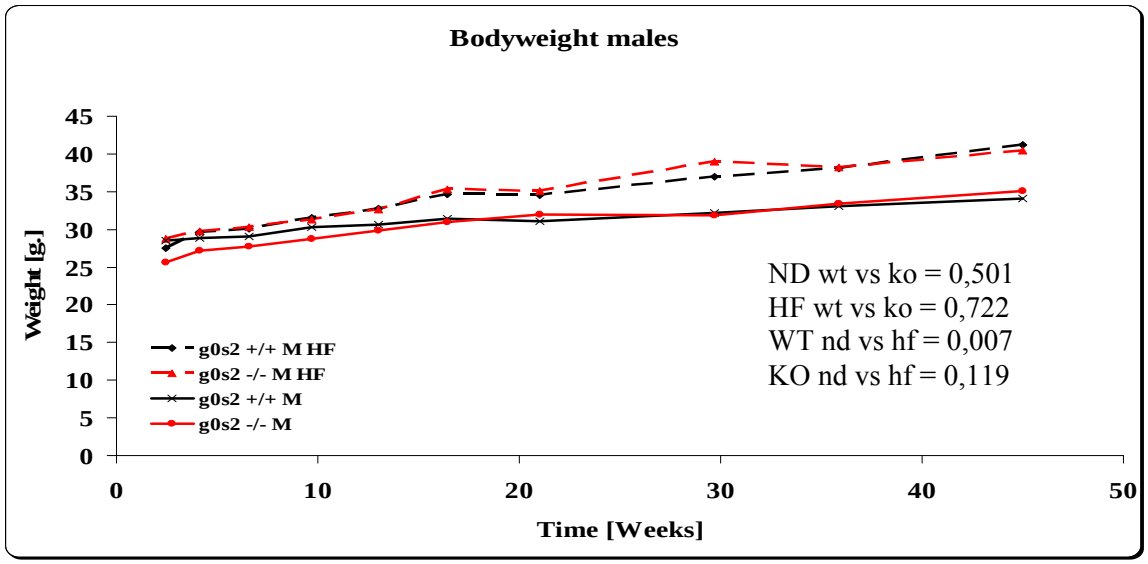

Figure 3.6: Bodyweight gain of mice fed in normal and high fat diet regime. Body weight gain on high fat diet was **s**hown for females **(A)** and males **(B)** The mice were put on 30% high fat diet (ssniff from Germany) rich food at age of 12 weeks. The body weight was measured for a period of 12 months. Data show means ± SEM of n= 4-10 per group.

BAY (1µM of 4-isopropyl-3-methyl-2-[1-(3-(S)-methyl-piperidin-1-yl)-methanoyl]-2H-isoxalo-5-one) was added. These experiments showed that ATGL activity was higher in adipose tissue derived from *g0s2*$^{-/-}$ mice compared to adipose tissue derived from *g0s2*$^{+/+}$ mice. Furthermore, in the presence of ATGL activator CGI-58 and HSL inhibitor, the ATGL activity remains significantly higher in adipose tissue derived from *g0s2*$^{-/-}$ mice

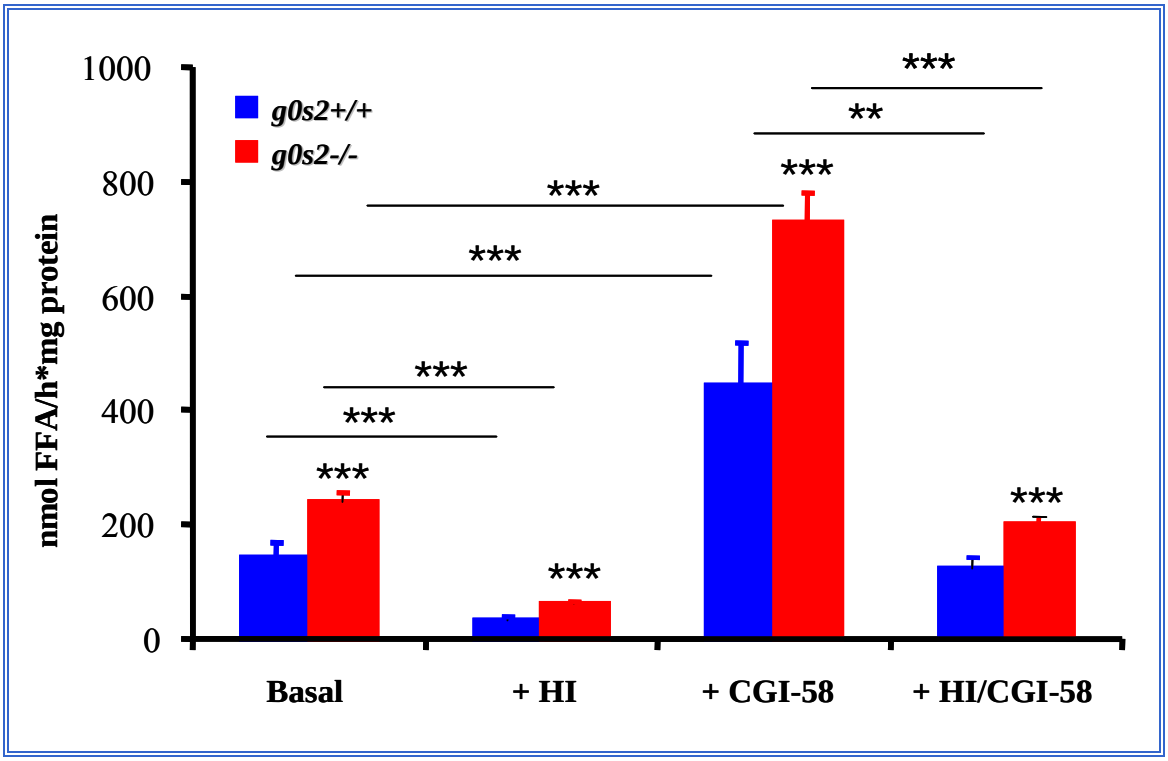

Figure 3.7: G0s2 deletion increases adipose triglyceride lipase activity (ATGL) in white adipose tissue. ATGL activity is measured in the presence of ATGL activator CGI-58 and hormone sensitive lipase inhibitor (4-isopropyl-3-methyl-2-[1-(3-(S)-methyl-piperidin-1-yl)-methanoyl]-2H-isoxalo-5-one (BAY) and in the presence of both HSL inhibitor and ATGL activator. Results are represented as mean ± SEM. (n=8). Abbreviation: HI- Hormone sensitive lipase inhibitor, CGI-58- Comparative gene identification protein-58.

compared to *g0s2*$^{+/+}$ mice (Fig.3.7). Similarly, the increase in ATGL activity in *g0s2*$^{-/-}$ mice increases the HSL activity indirectly (Fig.3.7) due to release of diacylglycerol produced by the ATGL lipolysis activates HSL. The results showed that g0s2 regulates lipolysis by inhibiting the activity of adipose triglyceride lipase in adipose tissue under *in vitro* condition. Next I analyzed the lipolysis under *in vivo* condition by measuring plasma free fatty acid and glycerol level following basal and overnight starvation in *g0s2*$^{-/-}$ mice compared to *g0s2*$^{+/+}$ mice. There was no difference in plasma free fatty acid and glycerol levels between the two cohorts (Fig.3.8. A,B). Similarly, plasma free fatty acid and glycerol levels of mice fed on high fat diet showed no difference under basal or in response to 16h starvation (data not shown)

A

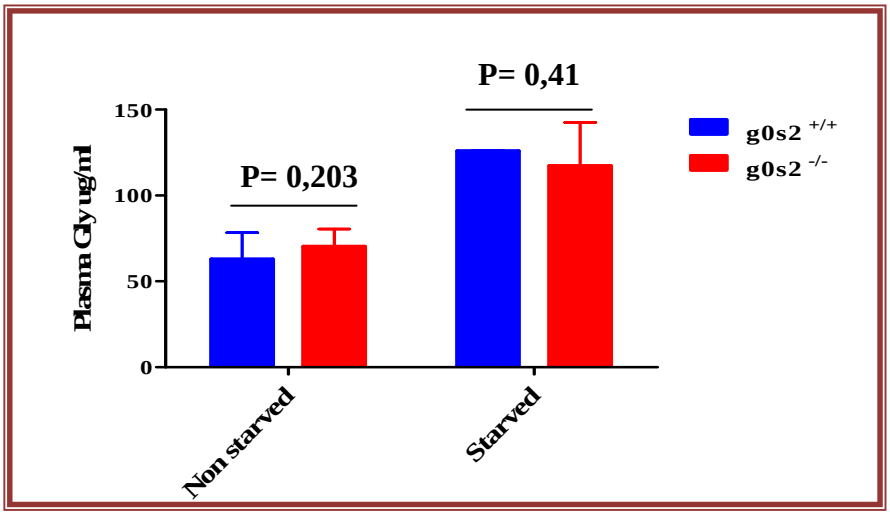

B

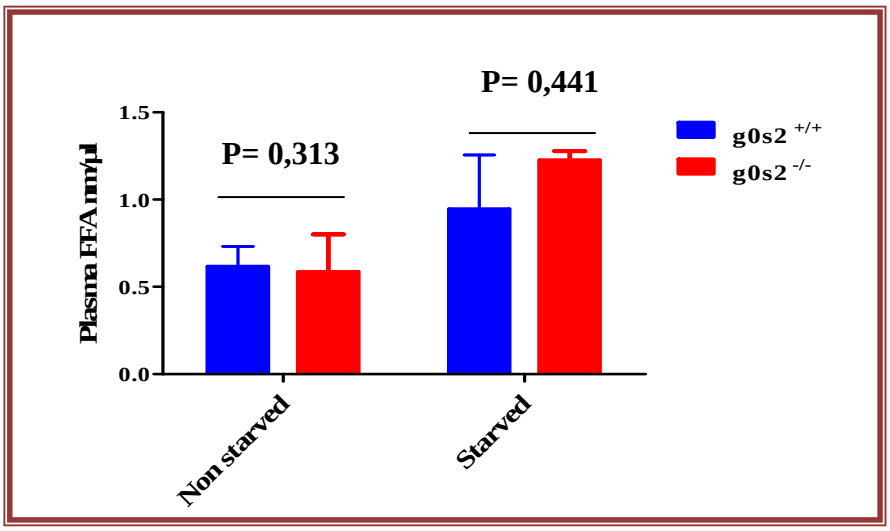

Figure 3.8: G0S2 deletion does not alter plasma free fatty acid or glycerol levels in mice on normal diet or in response to starvation. A-B. Bar graphs showing means ± SEM of the concentration of plasma free fatty acid and glycerol level under basal and 16h starvation (n=5). Mice were starved for overnight (16h) and plasma fatty acid and glycerol were quantified.

Previous studies have shown that lipolysis can be induced *ex vivo* on adipose tissue explants by isoproterenol and forskolin stimulation (75). Forskolin activates adenylate cyclase and isoproterenol stimulates β-adrenergic receptors leading to the activation of CGI-58, which inturn activates ATGL by competing with G0S2. Interestingly, stimulation of lipolysis on white adipose tissue fat explants by forskolin and

isoproterenol did not show any change in rate of lipolysis between *g0s2*$^{-/-}$ compared to controls and also between the sexes (data not shown). These results show that G0S2 deletion has no influence on the rate of lipolysis in adipose tissue compared to controls.

HF diet is used to induce obesity and diabetes in mouse. *G0s2* gene status did not influence the progression to diabetes in mice fed with a high fat diet as analysed by the oral glucose tolerance test (Fig.3.9.A-D) and insulin tolerance test (data not shown).

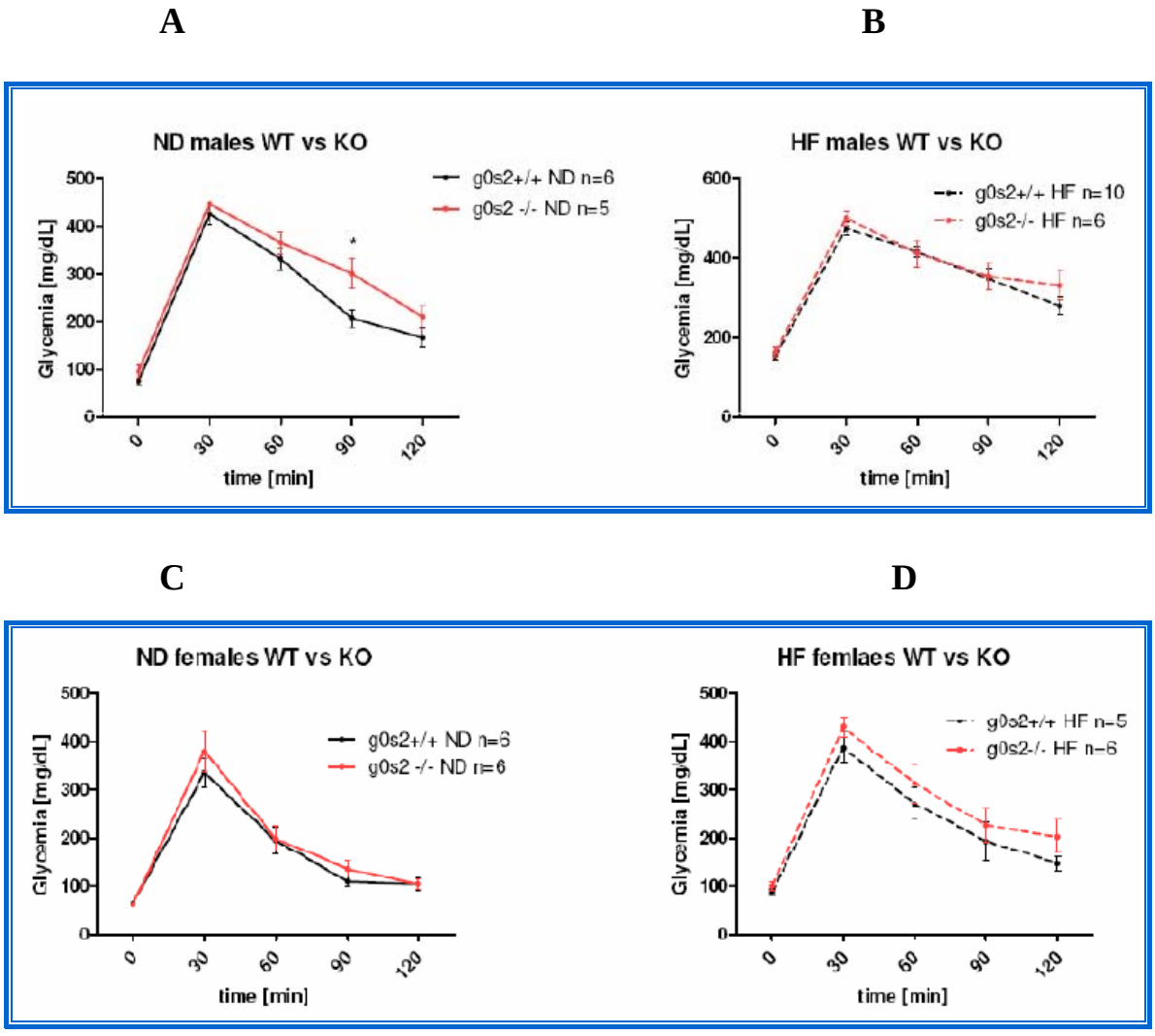

Figure 3.9: G0S2 gene status does not influence the development of diabetes in mice exposed to high fat diet. A-D. Results of oral glucose tolerance test (OGTT) from a g0s2$^{-/-}$ and control mice fed with normal and high fat diet fed with seven months. **A.** OGTT of 7 months old male mice fed on normal diet: B. OGTT of 7 month old male mice fed for 7 month with high fat diet: C. OGTT of 7 month old female mice fed on normal diet: D. OGTT of 7 month old female mice fed for 7 months with high fat diet. Data show means as ± SEM.

3.5 *G0s2* deletion improves liver regeneration after starvation

Liver is a highly quiescent organ that synchronously responds to injury by initiating cell cycle for organ mass regeneration. Previously it was found that mice undergoing partial hepatectomy, exhibit lipid deposition in the regenerating liver (110). Moreover the impaired regeneration of liver in starved mice was postulated to be due to increased fat deposition in liver (111).

Previously shown that starvation delays liver regeneration and the accumulation of fat in liver was shown to inhibit liver regeneration (66, 112). It was postulated that transient increases in hepatic fat content in response to starvation and lipolysis of peripheral fat depots may impair liver regeneration in response to starvation (111). However, this concept was never experimentally verified. I wished to analyze whether g0s2 could be involved in this process.

First, I analyzed the expression of g0s2 mRNA and protein in liver under

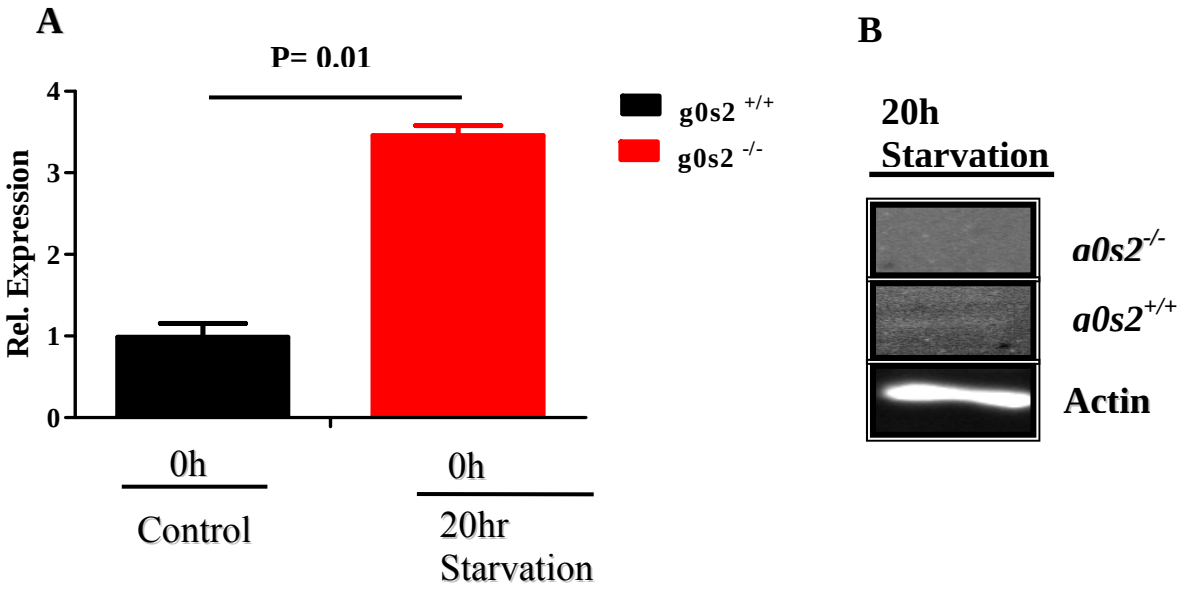

Figure 3.10: Real time PCR and Western blot analysis of g0s2 expression in liver after starvation. A. Real time PCR analysis of whole liver biopsies was performed with a Taqman probe (applied Bio-system) specific to g0s2 mRNA. **B.** Western blot analysis shows that expression of g0s2 protein in liver following 20h starvation. G0S2 proteins were detected using rabbit polyclonal antibody at 1:1000 dilution from Santa Cruz.

basal diet and 20h after food starvation. Quantitative PCR analysis revealed that g0s2 mRNA sharply increases 20h after starvation compared to mice exposed to normal diet. The g0s2 protein expression was undetectable in liver of mice exposed to normal diet but a weak band became detectable 20h after starvation (Fig.3.10).

To test whether g0s2 expression would influence liver regeneration in response to partial hepatectomy (PH), I analysed hepatocyte proliferation in *g0s2*$^{+/+}$ and *g0s2*$^{-/-}$ mice that were fed ad libitum (complete free access to food) or were starved for 20h prior to 2/3 part PH, following PH all mice were fed ad libitum (Fig.3.11). At 48h after PH, liver regeneration was similar in ad libitum fed mice independent of *G0S2* gene status as measured by staining for the proliferation marker "proliferating cell nuclear antigen" (PCNA). In agreement with previous studies, the starvation of *g0s2*$^{+/+}$ mice significantly

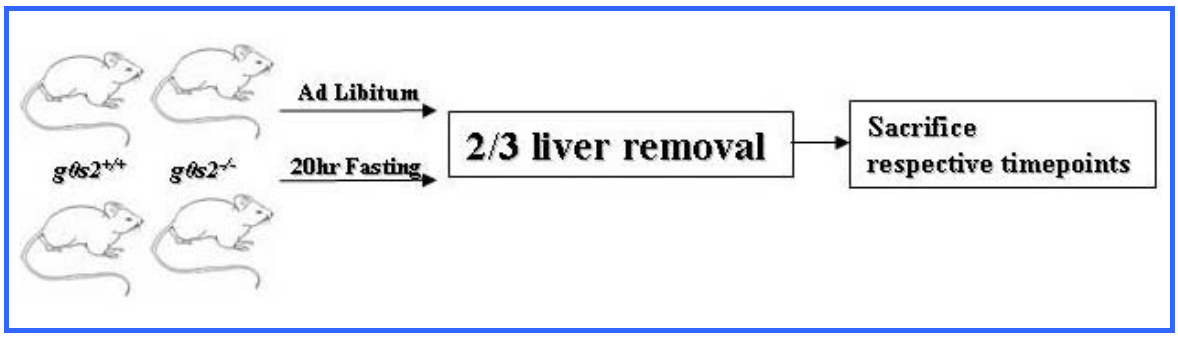

Figure 3.11: Scheme of liver regeneration. Mice were kept on free access to the food (ad libitum) and water or starved for 20h before partial hepatectomy (PH). After PH mice were sacrificed at 0h, 36h and 48h after starvation.

decreased proliferation rates as compared to ad libitum fed mice at 48h after PH as shown by the PCNA staining (Fig.3.12.A, C). Whereas 36h after PH represent an early time point when hepatocytes begin to enter the cell cycle after PH. At this time point, livers from starved *g0s2*$^{-/-}$ mice displayed already PCNA positive hepatocytes (Fig.3.12.B, C) whereas livers from starved *g0s2*$^{+/+}$ mice showed a reduced PCNA induction. This trend in PCNA expression differences at 36h after PH was not significant. However, liver regeneration in *g0s2*$^{-/-}$ was significantly improved with the 20hr period of starvation compared to wild type

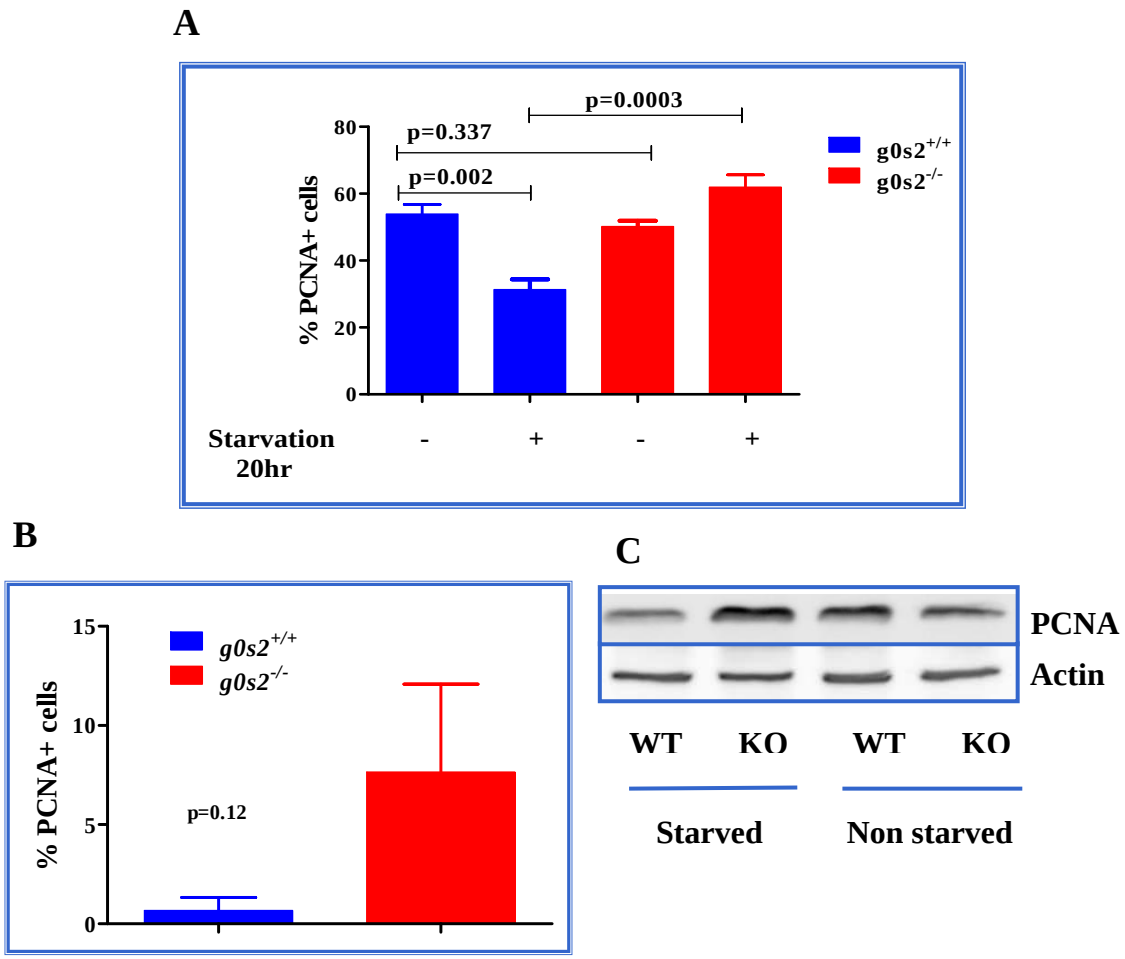

Figure 3.12: G0S2 limits liver regeneration after fasting. A. The histogram shows the percentage of PCNA-positive liver cells at 48h after PH of mice of the indicated genotypes, exposed to the indicated diet intervention. Bar graphs show means ± SEM (n=3-5 per group). **B**. The histogram shows the percentage of PCNA-positive liver cells at 36h after PH of mice of the indicated genotypes. Mice were exposed to 20h starvation prior to PH. Bar graphs show means ± SEM (n=3-5 per group). **C.** Western blot analysis of liver showing PCNA levels at indicated time points after partial hepatectomy in mice that were fed ad libitum or fasted for 20h previous PH. Pooled samples (n=3-5 mice per group) were used for the analysis.

controls (Fig.3.12.A, C). *G0s2*$^{-/-}$ mice that were starved overnight had a slight but significant improved proliferation compared to *g0s2*$^{-/-}$ mice that were fed ad libitum.

3.6 Fat deposition in liver is reduced in g0s2 knockout mice

Fat deposition in liver is a common event during liver regeneration and fasting. It was previously suggested that transient increase in fat deposition and lipolysis in starved mice is the cause of impaired liver regeneration.

Here, I evaluated the fat deposition in mice that underwent PH with or without exposure to a 20h fasting period prior to PH. Fat deposition were notably increased

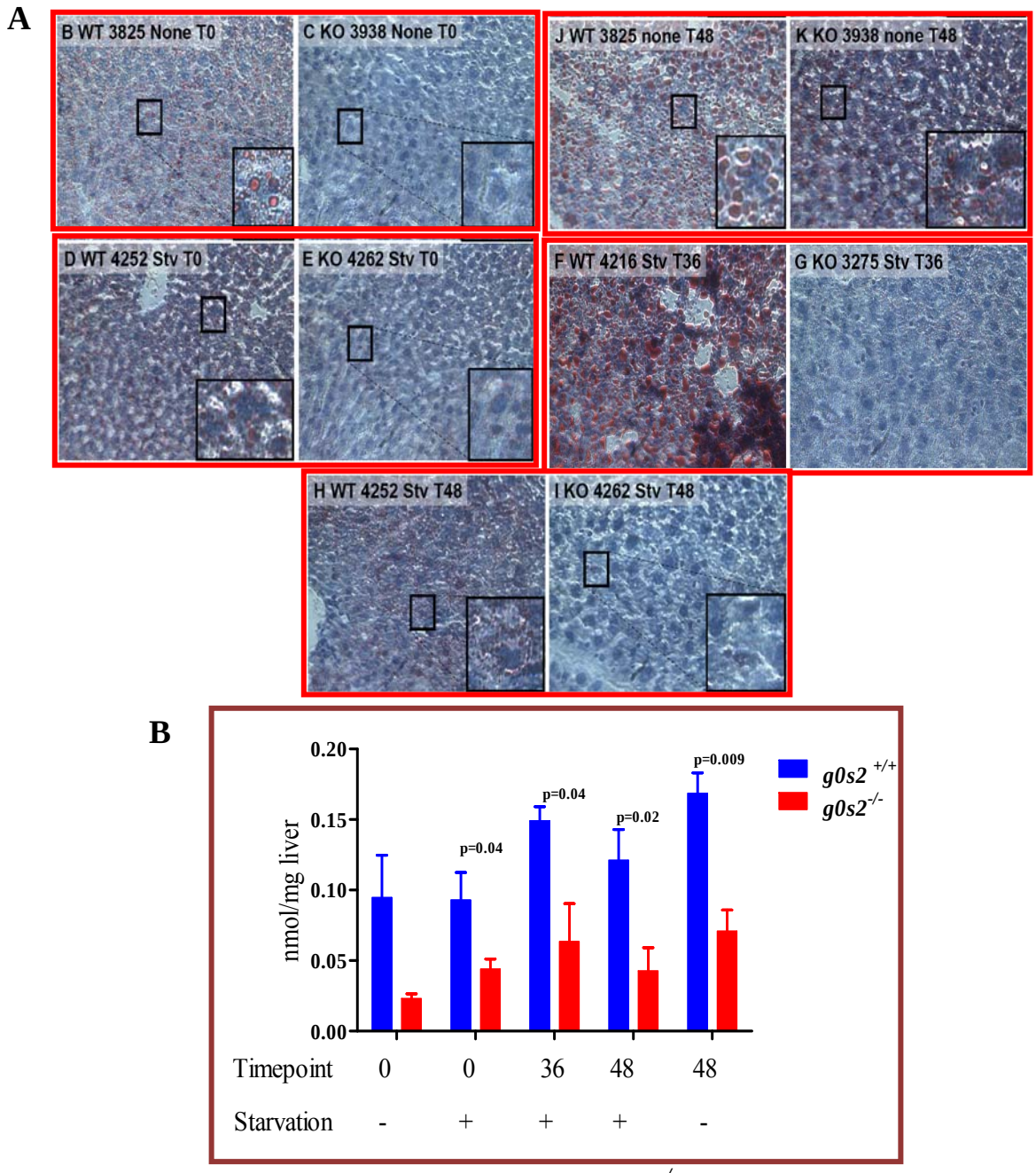

Figure 3.13: Fat deposition in liver is reduced in *g0s2*$^{-/-}$ mice. Partial hepatectomy was conducted in 2-3 month old mice fed ad libitum or fasted for 20h prior to PH. Mice had free access to food and water after PH and were sacrificed at the respective time points. **A.** Representative pictures of Oil red-O stained livers of *g0s2*$^{+/+}$ and *g0s2*$^{-/-}$ before and after PH with or without the fasting period. Note that *g0s2*$^{-/-}$ livers show reduction in lipid droplet formation in liver. **B.** The histogram shows the hepatic triglyceride content at the indicated time points after PH of mice of the indicated genotypes exposed to the indicated diet intervention. Bar graphs show mean value ± SEM, n=3-5 per group. Abbreviations: WT- Wild type (*g0s2*$^{+/+}$); KO- Knockout (*g0s2*$^{-/-}$).

with nonstarved and 0h starvation in *g0s2*$^{+/+}$ mice as observed by Oil red-O staining (Fig.3.13.A). Whereas *g0s2*$^{-/-}$ mice has less fat deposition in both nonstarvation and 0h starvation compared to *g0s2*$^{+/+}$ mice (Fig.3.13.A). Furthermore, the fat deposition after PH in *g0s2*$^{+/+}$ mice was notably increased at 36h and 48h as observed by Oil red O staining (Fig.3.13.A). Whereas in *g0s2*$^{-/-}$ mice fat deposition was significantly reduced at 36h and 48h after PH compared to *g0s2*$^{+/+}$ mice (Fig.3.13.A). However, this difference in fat deposition occurred at all investigated timepoint and was independent of the diet regiment.

Similar to oil-red O staining, haematoxylin and eosin staining showed that fat deposition was pronounced in *g0s2*$^{+/+}$ mice compared to *g0s2*$^{-/-}$ mice at 36h and 48h time points after PH, independent of the dietary intervention (data not shown). Then the quantification of fat in liver showed that under nonstarvation and starvation *g0s2*$^{+/+}$ liver significantly accumulates more fat than g0s2$^{-/-}$ liver at all investigated time points and was independent of the diet regiment (Fig.3.13.B). These results suggest that inhibition of liver regeneration after starvation in *g0s2*$^{+/+}$ mice could be independent of fat deposition but it may be associated with decreased utilization of deposited fat in *g0s2*$^{+/+}$ mice compared to g0s2$^{-/-}$ mice. To verify the hypothesis, I wished to study the expression of enzymes that regulate lipolysis with or without starvation.

It is well known that *g0s2* inhibits ATGL activity and ATGL is the primary lipase responsible for the degradation of TGs in liver. I analyzed the hepatic expression of Beclin, ATGL, HSL, and pHSL (ser565) levels under basal diet and after a 20h starvation period at 0h and 36h after PH.

Liver tissue from g0s2$^{-/-}$ showed an enhanced expression of ATGL compared to liver from *g0s2*$^{+/+}$ at all investigated time points, independent of the dietary intervention. More ATGL expression was seen at 36h after starvation in g0s2$^{-/-}$ mice

compared to *g0s2*$^{+/+}$ mice indicating the continuous acceleration of lipolysis in g0s2$^{-/-}$ mice. G0S2 gene status had no significant influence on HSL but more active form of HSL seen in 36h after starvation in g0s2$^{-/-}$ mice compared to *g0s2*$^{+/+}$ mice (Fig.3.14). The higher ATGL levels indirectly activates the HSL activity by producing diacyglycerol which is the

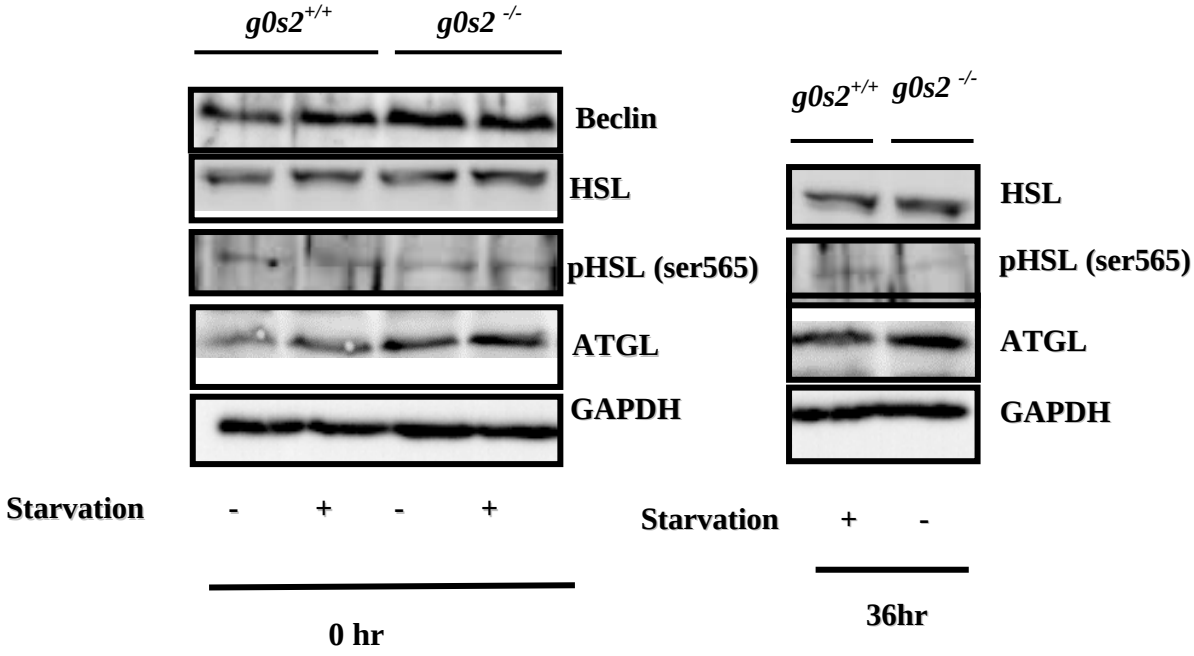

Figure 3.14: Western blot analysis shows the protein expression level of HSL, pHSL (ser 565) Beclin and ATGL (Cell Signalling dilution 1:1000) in liver tissue of mice of the indicated genotypes that were exposed to PH at the indicated time points. Mice were exposed to a starvation period of 20h prior to PH. Abbreviations: HSL-Hormone sensitive lipase; ATGL- Adipose triglyceride lipase; GAPDH- Glycerol 3-phosphate dehydrogenase.

necessary substrate for HSL. Together, higher ATGL levels and higher active HSL in liver of g0s2$^{-/-}$ mice correlated with increased lipolysis and reduced fat content in liver of g0s2$^{-/-}$ mice compared to *g0s2*$^{+/+}$ mice after PH. Autophagy is a process that normally provides essential energy via degradation of hepatic triglycerides during starvation (132, 135). Anaylsis of beclin mediated autophagy shows that g0s2$^{-/-}$ mice has more beclin levels following basal and 0hr starvation after PH compared to *g0s2*$^{+/+}$ mice. This result show that under starvation G0S2 deletion enhances the beclin mediated autophagy and thus may provide the energy for the cellular process.

3.7 Enhanced ATGL Activity Is Associated With Improved Liver Regeneration

Next, I measured ATGL activity of liver tissue from *g0s2*$^{+/+}$ and g0s2$^{-/-}$ mice. ATGL activity was measured in the presence and absence of ATGL activator CGI-58 and in the absence or presence of an HSL inhibitor (BAY). Analysis showed that there was a significant increase in the ATGL activity in liver of g0s2$^{-/-}$ compared to *g0s2*$^{+/+}$ mice (Fig.3.15). In addition, the higher ATGL activity indirectly increases the HSL activity by producing diacylglcerol from TG by ATGL hydrolysis (Fig.3.15).

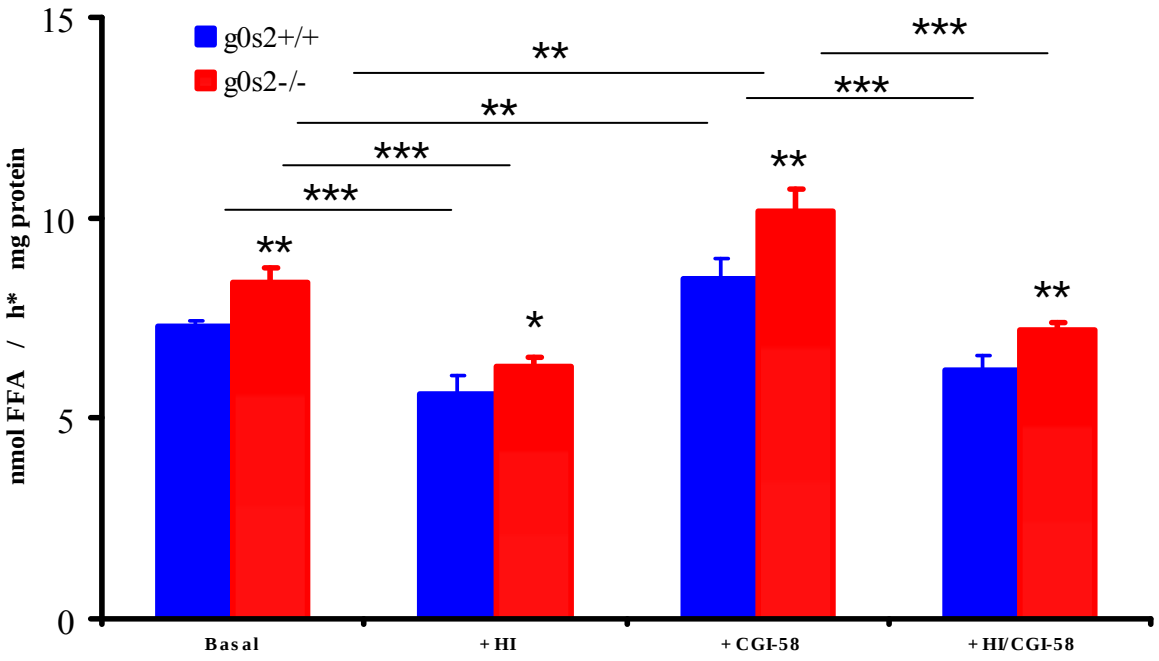

Figure 3.15: G0s2 deletion increases adipose triglyceride lipase activity (ATGL) in liver tissue. ATGL activity is measured in liver tissue of 2-3 month old mice of the indicated genotypes. Freshly isolated liver tissue was used for the *in vitro* analysis in the presence or absence of the ATGL activator (CGI-58), the HSL inhibitor (HI). Results are represented as mean ± SEM (n=8 mice per group).

These data supports the notion that increase in the ATGL activity in g0s2$^{-/-}$ mice could accelerates and thus may provide free fatty acids and glycerol for excessive energy production which is required for hepatocellular proliferation during regeneration and that this can be abolished with presence of G0S2 leading to inhibition of lipolysis.

3.8 *G0s2* inhibits cell cycle after starvation

To further evaluate whether the deletion of g0s2 promotes liver regeneration, we analysed the cell cycle regulators cyclin A, cdc2, p21 and p27 before and after starvation previous to the removal of 2/3 of liver. Cyclin A and cdc2 acts as positive regulators of cell cycle (113). Cyclin A is a member of cyclin family binds to S phase Cdk2 (114) and is required for the cell to progress through the S phase, whereas Cyclin A/ Cdk2 is inhibited by the complex p21CIP (115). Cdc2 is also known as cyclin-dependent kinase 1, this highly conserved protein is a key regulator of cell cycle by phosphorylating its targets leading to cell cycle progression (114). In contrast, p21 and p27 are negative regulators of cell cycle by inhibiting cyclin dependent kinases (115).

Expression analysis of cell cycle regulators Cdc2, cyclin A, and PCNA in response to starvation after PH shows that the transient up regulation of these proteins occur during liver regeneration. However, expression analysis of Cdc2, Cyclin A, and PCNA confirmed the reduced proliferative response in $g0s2^{+/+}$ mice at 48h after PH when mice were exposed to a 20h starvation period prior to PH compared to ad libitum fed mice (Fig.3.16). The increased liver regeneration in $g0s2^{-/-}$ mice is correlated with high expression of Cdc2, Cyclin A, and PCNA at 48h after PH compared to ad libitum fed mice (Fig.3.16). Similarly, the expression of cell cycle inhibitors, p21 and p27 level is increased at 0h and 36h after starvation in $g0s2^{+/+}$ mice (Fig.3.16). Furthermore, the expression of ATGL was reduced in $g0s2^{+/+}$ mice at all investigated time points compared to $g0s2^{-/-}$ mice (Fig.3.16). The decreased expression of ATGL, Cdc2, Cyclin A, PCNA and increased expression of p21 and p27 levels coupled with impaired liver regeneration in $g0s2^{+/+}$ mice compared to $g0s2^{-/-}$ mice. Whereas the improved liver regeneration in $g0s2^{-/-}$ mice correlated with increased expression of ATGL at all investigated time points and increased

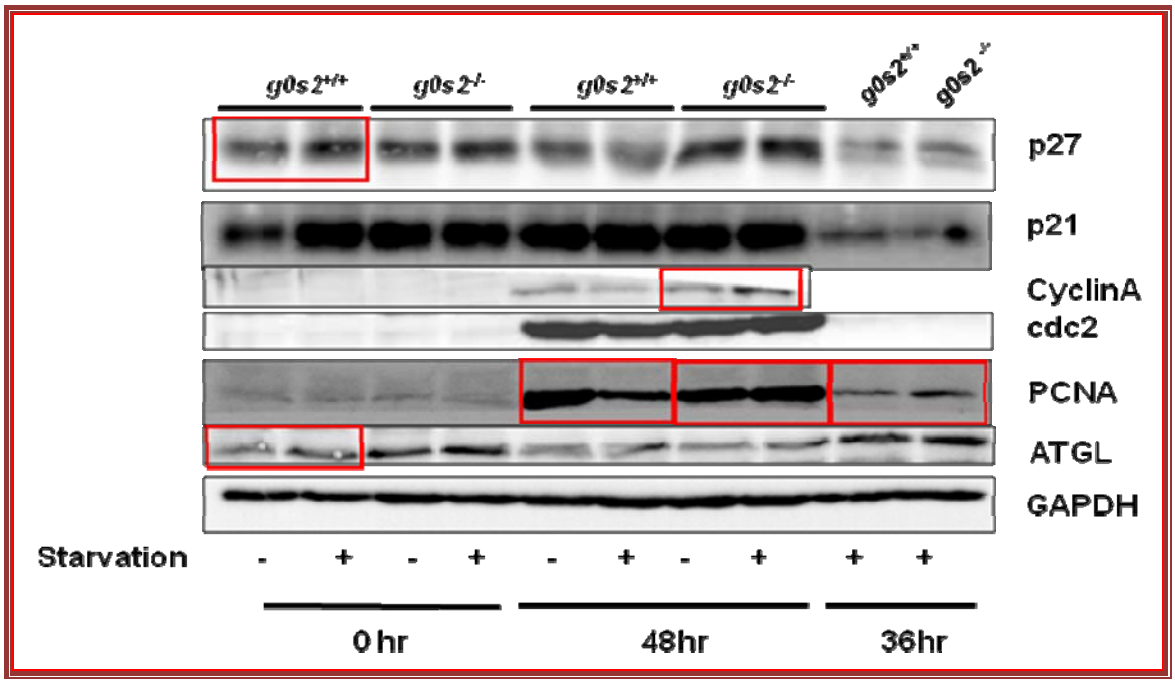

Figure 3.16: G0S2 inhibits cell cycle after fasting. Western blot analysis shows the expression of cell cycle regulatory proteins p21, p27, Cyclin A and cdc2 (All the antibodies are from cell signalling diluted to 1:1000) in liver tissue of mice of the indicated genotypes expose to the PH at the indicated timepoints. Starved mice were exposed to a starvation of 20h period prior to PH. 20µg of protein were loaded per well.

expression of positive cell cycle regulators Cdc2, Cyclin A, PCNA at 48h and decreased expression of cell cycle inhibitors p21 and p27 levels at 36h time point (Fig.3.16).

These results show that impaired liver regeneration in *g0s2*$^{+/+}$ mice is due to up regulation of g0s2 mRNA and protein level following starvation (Fig.3.10) and thus inhibit ATGL activity leads reduced lipolysis which inhibits the hepatocellular proliferation. Whereas in the absence of *g0s2* in g0s2$^{-/-}$ mice ATGL activity is more in basal state and ATGL activity is further enhanced in starvation leads to accelerated lipolysis which may facilitates hepatocellular proliferation by either may providing free energy and fatty acids or cellular membrane synthesis and other process. Thus, g0s2 acts as cell-cycle regulatory functions in liver involving its role in modulating fat metabolism in mice starvation. Supporting the notion that *g0s2* acting as a cell cycle inhibitor under certain conditions, over-expression of *g0s2* in the hematopoietic system improves stem cell

function and hematopoietic reconstitution by maintaining stem cell quiescence (16) and inhibiting their depletion during serial transplantation (data not shown).

4. Discussion

Previous studies have shown that G0S2 is essential for the *in vitro* differentiation of adipocytes in mouse 3T3-L1 fibroblast and human SGBS fibroblasts (37, 38) by a PPAR-γ dependent manner. A suggestive role of G0S2 as a tumor suppressor was proposed with the identification of its silencing in squamous lung carcinoma, endometrial cancer, lung and neck cancer (29-35). G0S2 was also shown to localize to mitochondria and stimulates apoptosis by interacting with Bcl-2 proteins though it lacks the Bcl-2 binding domain and preventing its ability to heterodimerize with Bax in HeLa cells (28). Probably the most prominent function of G0S2 was identified in regulating fat metabolism. G0S2 was shown to inhibit the adipose triglyceride lipase ATGL (54) and G0S2 binds to ATGL irrelevantly of its activity state (66) and biochemical characterisation of G0S2 revealed that hydrophobic domain of G0S2 binds with patatin N-terminal domain of ATGL (59) and attenuates ATGL activity by competing with CGI-58 (20). In addition, G0S2 co-localizes with ATGL on the surface of lipid droplet and inhibit lipolysis of TGs. The knockdown of endogenous G0S2 accelerates basal and stimulated lipolysis in adipose tissue, whereas over expression of G0S2 reduces the rate of lipolysis in both adipose tissue explants and adipocytes (20).

Based on the previous studies, we expected G0S2 could play a role in an *in vivo* setting of adipogenesis, cellular proliferation, cell survival and prognosis of type 2 diabetes. To address the *in vivo* function of G0S2, I investigated the phenotypic consequences of g0s2 deletion in a newly generated knockout mouse model. We observed that deletion of *g0s2* is dispensable for embryonic development, the maintenance of adult tissues with aging. *G0S2* deleted mice exhibited normal organ development, organ weights and blood counts of red blood cells (RBC), white blood cells (WBC) and platelets and during the observation period no overt phenotype was observed. Our study provides the

first evidence for the role of G0S2 in liver regeneration by regulating ATGL.

It was demonstrated that G0S2 localize to mitochondria and stimulates apoptosis by interacting with Bcl-2 proteins in HeLa cells. In contrast, our study shows that g0s2 deleted thymocytes has unchanged apoptosis and no difference in the survival of irradiated mice. Our results showed the less importance of g0s2 in inducing apoptosis in thymocytes.

In contrast to the previous reports, adipogenesis induction of g0s2 deleted fibroblasts, although slightly diminished, was not significantly affected compared to wild type fibroblasts when Oil Red-O deposition was quantified suggesting the less importance of G0S2 in adipogenesis.

As it was shown that g0s2 is important regulator of lipolysis by directly inhibiting ATGL activity and responsible for maintenance of lipid droplet integrity in adipose tissue, the deletion of g0s2 did not significantly affected the body weight and white adipose tissue content. Furthermore, the plasma free fatty acid and glycerol release following basal and starvation did not show any change in rate of lipolysis in g0s2-deleted mice compared to wild type mice. Similarly, ex vivo induction of lipolysis on white adipose tissue explants by isoproterenol and forskolin stimulation do not show any change in rate of lipolysis in $g0s2^{-/-}$ white adipose tissue explants. The results show that g0s2 is less important in regulating lipolysis in adipose tissue.

Studies on mouse models of obesity and human obesity showed a decrease in G0S2 levels in white adipose tissue in response to TNF-α signalling (24, 25). In human obesity, decreased G0S2 expression in adipose tissue leads to increased plasma free fatty acids and thus responsible for development of insulin resistance and type 2 diabetes (84). Our study provides evidence that g0s2 deletion does not induce diabetes under normal diet

and high fat diet as shown by oral glucose tolerance test (OGTT) and insulin tolerance test. These results suggest that G0S2 has not a major role in the pathogenesis of type II diabetes.

The fine line between beneficial and detrimental steatosis during liver regeneration is a matter of discussion. While steatosis in obese mice causes impaired liver regeneration (104), abolishment of lipid droplet formation in mice also diminishes regenerative potential of hepatocytes (105, 100). The implications of liver regeneration get more complex considering the impairment in liver regeneration during a period of starvation (106). Vilchez et al (106), proposed two reasons for this phenomenon to occur: i) because of the lack of food or energy per se leads to impaired regeneration, ii) or the excessive lipid infiltration that occurs during starvation and this accumulation of lipids impairs regeneration.

Our study suggests that impairment of liver regeneration in response to starvation is rescued by G0S2 gene deletion. We found that ATGL activity is significantly increased in liver of *g0s2*$^{-/-}$ mice compared to wild type mice. Previous studies have shown that over-expression of ATGL and HSL in liver promotes β-oxidation of fatty acids by increasing plasma 3-beta-hydroxybutyrate levels and stimulate direct release of free fatty acid and ameliorate hepatic steatosis in high fat induced obesity and *ob/ob* mice (111). It is possible that the increase in ATGL activity in liver of G0S2 knockout mice prevents starvation-induced impairments in liver regeneration that occur in wild type mice. However, this interpretation is flawed by the fact that we did not see a significant increase in hepatic steatosis of wild type mice in response to starvation in our experiments. These findings suggest that G0S2 may have other effects on liver regeneration in starved mice that do not directly correlate to the level of steatosis. One possibility is that G0S2 influence

liver regeneration via regulating PPAR-alpha signalling.

Previous studies revealed that the activity of PPAR-α requires its ligands, heterodimerization and coactivation by PGC-1α or PGC-1β (45). PGC-1α or PGC-1β expressions are the indicators of mitochondrial respiration and biogenesis (116-118). ATGL hydrolysis produces the ligands for PPAR-activation and its target genes and $ATGL^{-/-}$ mice exhibit decreased expression of PPAR-α and PPAR-δ target genes in heart leading to decreased PGC-1α and PGC-1β expression inhibition of mitochondrial oxidation and leading to cardiomyopathy (45).

It was demonstrated that in response to starvation G0S2 expression decreases in adipose tissue but increases in liver (21, 25, 80). This differential regulation of G0S2 under starvation may regulate the redistribution of free fatty acids released by adipose tissue to the liver. During fasting the liver cannot keep up the excess FFA influx by increasing the very low density lipoprotein production and β-oxidation of fatty acids. Thus, G0S2 may play an important role in preventing the potential cytotoxic effects of excess free fatty acids release by facilitating fatty acid in to lipid droplet formation in the liver and tightly regulating the breakdown of TGs. The cytotoxic effects of free fatty acids include enhancing the cell damaging reactive oxygen (ROS) species production and impairment of insulin sensitivity by stimulating the insulin secretion. Evidence from previous study showed that lipolysis was essential for the synthesis of fatty acid derived ligands or precursors of ligands for PPARα in liver (45, 119-121). Therefore, even though there is a marked increase in G0S2 expression in liver during starvation, endogenous G0S2 may need to be delicately controlled so that sufficient ATGL activation would still allow to mediate PPARα activation and FA oxidation.

The excessive accumulation of lipids at the end would have detrimental

rather than beneficial effects as previously suggested in model of pathologic liver steatosis. Moreover, our study shows that g0s2 inhibits the lipolysis of fat in liver. Our study shows that g0s2 deletion enhances the ATGL activity and improves liver regeneration after starvation. These data have an important implications since the metabolic effect in liver occurs without causing other effects in adipose tissues or organ homeostasis in g0s2$^{-/-}$ mice. Reasons for decreased fat deposition in the liver of g0s2$^{-/-}$ starved mice could be the accelerated lipolysis of newly formed fat droplets probably by ATGL. Supporting this hypothesis is that over-expression of ATGL in liver considerably increases the lipolysis of fat in livers of obese mice (111). G0S2 is up regulated in liver under starvation (80) and presumably inhibits ATGL. Although the spectrum of organs where ATGL deletion has an effect also includes the liver (65), the levels of ATGL in liver seem to be low or undetectable as compared to those in adipose tissue (112, 122, 123). Previously it was demonstrated that G0S2 localize to mitochondria (15, 16) and this piece of evidence suggests that g0s2 might control other players responsible for fatty acid oxidation in liver mitochondria. Reduced liver regeneration is observed in mice that cannot form lipid droplets (100). Our study shows that G0S2 deletion does not lead to an abrogation of lipid import into liver or a complete block of lipid droplet formation. Instead, our study suggests improved lipolysis (lipid droplet degradation) in liver of starved *g0s2*$^{-/-}$ mice may also lead to improved energy usage that is translated in accelerated liver regeneration. Nonetheless, the data on adipogenesis in white adipose tissue suggest that there is an exquisite regulation of lipid metabolism via g0s2 in liver but not other organs.

For the effective growth and differentiation, a cell needs both energy and substrates for membrane synthesis. Lipolysis of triglycerides by ATGL provides the free fatty acids that can be utilised for membrane synthesis and energy production through

oxidation of free fatty acids. Previously it was shown that the ATGL homologue in yeast *Tgl4*, is phosphorylated and activated by the cyclin dependenk kinase 1 Cdk1/cdc28 and thus quiescent yeast enter the cell cycle by hydrolysing TGs and providing fatty acids for cellular proliferation (124). The activation of Tgl4 is necessary for full cell cycle initiation as the *Tgl4* mutant exhibits delay in bud formation (124). This study linked for the first time cell cycle progression with lipid metabolism in the yeast system (125). While the Tgl4 mutant yeast has delayed bud formation, it remains elusive whether the lethality of the ATGL knockout mouse is only due to excessive lipid deposition and not to cell cycle deregulation in certain cellular compartments. It is possible that deletion of g0s2 contributes to increase in ATGL mediated lipolysis, which in turn makes the free fatty acids and its ligands available for proliferation under starvation. Previous evidence showed dual roles of cell cycle regulators in the control of both proliferation and metabolic process (126). It was demonstrated previously that in response to activation of proliferation, cdk-pRB-E2F complex facilitate switch from oxidative to glycolytic metabolism and provides the glycolytic products to fatty acid synthesis (127-129).

It was demonstrated that G0S2 is up regulated when cells enter from the G0 stage of cell cycle into G1 phase of the cell cycle (18). Moreover, Yamada et al showed that G0S2 maintains quiescence of hematopoietic stem cells by sequestration of nucleolin in the cytosol (87). Nucleolin is a multifunctional protein present in the nucleolus, nucleoplasm, cytosol and at the cell surface (130). Nucleolin enhances cell growth by regulating the transcription of ribosomal DNA in the nucleolus, maturation of pre-ribosomal RNA, transport of ribonucleoproteins and ribosomal particles to the cytosol for final assembly (131). In addition, nucleolin stabilizes mRNA, enhances translation, and shuttles proteins into the nucleus (132–134). Nucleolin's ability to increase protein

biosynthesis and cell mass suggests that this protein may also help to control the cell cycle. It could be possible that impairment of liver regeneration due to up regulation of G0S2 under starvation could sequester the nucleolin and thus inhibiting its function necessary for cell growth. Further studies are required to dissect the involvement of G0S2 in other cellular growth process like synthesis of proteins, stabilization of mRNA and maturation, transport of ribonucleoproteins and ribosomal particle to the cytoplasm.

Here I propose the model (Fig 4.1) for G0S2 mediated cell proliferation in response to basal and starvation condition. In addition, G0S2 may shuttle the free glycerol

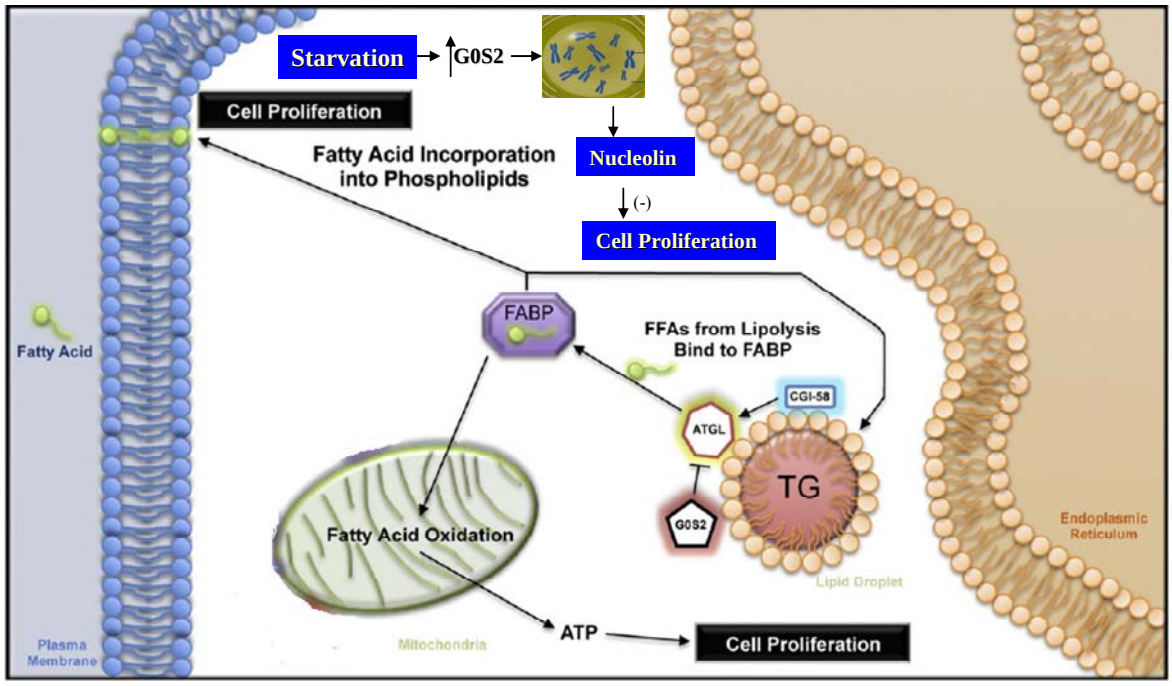

Figure 4.1: Cell Cycle Regulation by G0S2 in liver. In response to starvation to G0S2 is up regulated and thus facilitates the retention of nucleolin in to cytoplasm and inhibits cell proliferation. Alternatively, G0S2 controls cell proliferation by controlling ATP and ribose production by inhibiting ATGL. Figure modified from (135)

released by lipolysis in to pentose phosphate pathway for ribose sugar synthesis, which is necessary for the synthesis of DNA.

One cannot rule out the hormonal influence on ATGL and HSL action under basal and starvation conditions. It is well known that under fed condition insulin

stimulates lipogenesis by activating fatty acid synthase and inhibits lipolysis by inhibiting protein kinas A activation (136). In contrast, under starvation epinephrine activates the adenylate cyclase and stimulates lipolysis by activating hormone sensitive lipase, perilipin A and CGI-58 which in turn activates ATGL (136, 27). Previously, it was hypothesised that ATGL exist in both phosphorylated and dephosphorylated forms. Under basal condition, dephosphorylated-ATGL is present in both in the cytosol and on the surface of the lipid droplets mediating basal lipolysis (27), where as starvation may mediate the phosphorylation of ATGL thus enhancing its lipolytic activity. It was demonstrated that fasting epinephrine deficient mice develop liver steatosis and the mice exhibit impaired hepatic autophagy (137, 138) a process that normally provides essential energy via degradation of hepatic triglycerides during starvation. Our study shows that under starvation G0S2 deletion enhances the beclin expression suggesting that beclin-mediated autophagy may be increased and may provide energy for cellular processes in liver.

Together our studies indicate that G0S2 regulates lipid metabolism in liver by influencing ATGL activity. This regulation may be involved in G0S2-dependent effects inhibiting liver regeneration under starvation conditions. However, our measurement of triglyceride lipids in liver did not show a significant correlation between impaired liver regeneration and triglyceride accumulation in liver of starved wild type mice compared to ad libitum fed mice. It is possible that other metabolites are involved, e.g. free fatty acid. Our study provides the first *in vivo* evidence that G0S2 is an important regulator of lipid metabolism and cell cycle activity in liver. Importantly, the study also shows that G0S2 is dispensable for adipogenesis in adipose tissues indicating that G0S2 may have tissue specific roles.

1. Segrest, J.P., Jones, M.K., De Loof, H. & Dashti, N. Structure of apolipoprotein B-100 in low density lipoproteins. *J Lipid Res* **42**, 1346-1367 (2001).
2. Hunter, J.E. Dietary trans fatty acids: review of recent human studies and food industry responses. *Lipids* **41**, 967-992 (2006).
3. Teno, S., *et al.* Association of postprandial hypertriglyceridemia and carotid intima-media thickness in patients with type 2 diabetes. *Diabetes Care* **23**, 1401-1406 (2000).
4. Tushuizen, M.E., Diamant, M. & Heine, R.J. Postprandial dysmetabolism and cardiovascular disease in type 2 diabetes. *Postgrad Med J* **81**, 1-6 (2005).
5. Rader, D.J. & Daugherty, A. Translating molecular discoveries into new therapies for atherosclerosis. *Nature* **451**, 904-913 (2008).
6. Taskinen, M.R. Diabetic dyslipidaemia: from basic research to clinical practice. *Diabetologia* **46**, 733-749 (2003).
7. Hanson, R.W. & Reshef, L. Glyceroneogenesis revisited. *Biochimie* **85**, 1199-1205 (2003).
8. Shi, Y. & Burn, P. Lipid metabolic enzymes: emerging drug targets for the treatment of obesity. *Nat Rev Drug Discov* **3**, 695-710 (2004).
9. Bouchard, C., *et al.* Long-term exercise training with constant energy intake. 1: Effect on body composition and selected metabolic variables. *Int J Obes* **14**, 57-73 (1990).
10. Lewis, G.F., Carpentier, A., Adeli, K. & Giacca, A. Disordered fat storage and mobilization in the pathogenesis of insulin resistance and type 2 diabetes. *Endocr Rev* **23**, 201-229 (2002).
11. Samra, J.S. Sir David Cuthbertson Medal Lecture. Regulation of lipid metabolism in adipose tissue. *Proc Nutr Soc* **59**, 441-446 (2000).
12. Samra, J.S., Clark, M.L., Humphreys, S.M., Macdonald, I.A. & Frayn, K.N. Regulation of lipid metabolism in adipose tissue during early starvation. *Am J Physiol* **271**, E541-546 (1996).
13. Sternson, S.M. Metabolism: Let them eat fat. *Nature* **477**, 166-167 (2011).
14. Cahill, G.F., Jr. Fuel metabolism in starvation. *Annu Rev Nutr* **26**, 1-22 (2006).
15. Welch, C., *et al.* Identification of a protein, G0S2, that lacks Bcl-2 homology domains and interacts with and antagonizes Bcl-2. *Cancer Res* **69**, 6782-6789 (2009).
16. Yamada, T., Park, C.S., Burns, A., Nakada, D. & Lacorazza, H.D. The cytosolic protein G0S2 maintains quiescence in hematopoietic stem cells. *PLoS One* **7**, e38280 (2012).
17. Bachner, D., *et al.* Bmp-2 downstream targets in mesenchymal development identified by subtractive cloning from recombinant mesenchymal progenitors (C3H10T1/2). *Dev Dyn* **213**, 398-411 (1998).

18. Russell, L. & Forsdyke, D.R. A human putative lymphocyte G0/G1 switch gene containing a CpG-rich island encodes a small basic protein with the potential to be phosphorylated. *DNA Cell Biol* **10**, 581-591 (1991).

19. Heximer, S.P. & Forsdyke, D.R. A human putative lymphocyte G0/G1 switch gene homologous to a rodent gene encoding a zinc-binding potential transcription factor. *DNA Cell Biol* **12**, 73-88 (1993).

20. Teunissen, B.E., *et al.* Activation of PPARdelta inhibits cardiac fibroblast proliferation and the transdifferentiation into myofibroblasts. *Cardiovasc Res* **75**, 519-529 (2007).

21. Zandbergen, F., *et al.* The G0/G1 switch gene 2 is a novel PPAR target gene. *Biochem J* **392**, 313-324 (2005).

22. Kitareewan, S., *et al.* G0S2 is an all-trans-retinoic acid target gene. *Int J Oncol* **33**, 397-404 (2008).

23. Parikh, H., *et al.* TXNIP regulates peripheral glucose metabolism in humans. *PLoS Med* **4**, e158 (2007).

24. Austin, S., *et al.* Induction of the nuclear orphan receptor RORgamma during adipocyte differentiation of D1 and 3T3-L1 cells. *Cell Growth Differ* **9**, 267-276 (1998).

25. Harkness, R.D. Regeneration of liver. *Br Med Bull* **13**, 87-93 (1957).

26. Nielsen, T.S., *et al.* Fasting, but not exercise, increases adipose triglyceride lipase (ATGL) protein and reduces G(0)/G(1) switch gene 2 (G0S2) protein and mRNA content in human adipose tissue. *J Clin Endocrinol Metab* **96**, E1293-1297 (2011).

27. Yang, X., *et al.* The G(0)/G(1) switch gene 2 regulates adipose lipolysis through association with adipose triglyceride lipase. *Cell Metab* **11**, 194-205 (2010).

28. Cristillo, A.D., Heximer, S.P., Russell, L. & Forsdyke, D.R. Cyclosporin A inhibits early mRNA expression of G0/G1 switch gene 2 (G0S2) in cultured human blood mononuclear cells. *DNA Cell Biol* **16**, 1449-1458 (1997).

29. Chang, X., *et al.* Identification of hypermethylated genes associated with cisplatin resistance in human cancers. *Cancer Res* **70**, 2870-2879 (2010).

30. Kusakabe, M., *et al.* Identification of G0S2 as a gene frequently methylated in squamous lung cancer by combination of in silico and experimental approaches. *Int J Cancer* **126**, 1895-1902 (2010).

31. Kusakabe, M., *et al.* Impact of DNA demethylation of the G0S2 gene on the transcription of G0S2 in squamous lung cancer cell lines with or without nuclear receptor agonists. *Biochem Biophys Res Commun* **390**, 1283-1287 (2009).

32. Tokumaru, Y., *et al.* Inverse correlation between cyclin A1 hypermethylation and p53 mutation in head and neck cancer identified by reversal of epigenetic silencing. *Cancer Res* **64**, 5982-5987 (2004).

33. Ma, Y., *et al.* Microarray analysis uncovers retinoid targets in human bronchial epithelial cells. *Oncogene* **22**, 4924-4932 (2003).

34. Cheng, Y.H., Utsunomiya, H., Pavone, M.E., Yin, P. & Bulun, S.E. Retinoic acid inhibits endometrial cancer cell growth via multiple genomic mechanisms. *J Mol Endocrinol* **46**, 139-153 (2011).

35. Kersten, S., Desvergne, B. & Wahli, W. Roles of PPARs in health and disease. *Nature* **405**, 421-424 (2000).

36. Mandard, S., Muller, M. & Kersten, S. Peroxisome proliferator-activated receptor alpha target genes. *Cell Mol Life Sci* **61**, 393-416 (2004).

37. Tontonoz, P., Hu, E. & Spiegelman, B.M. Stimulation of adipogenesis in fibroblasts by PPAR gamma 2, a lipid-activated transcription factor. *Cell* **79**, 1147-1156 (1994).

38. Barak, Y., *et al.* PPAR gamma is required for placental, cardiac, and adipose tissue development. *Mol Cell* **4**, 585-595 (1999).

39. Ren, D., Collingwood, T.N., Rebar, E.J., Wolffe, A.P. & Camp, H.S. PPARgamma knockdown by engineered transcription factors: exogenous PPARgamma2 but not PPARgamma1 reactivates adipogenesis. *Genes Dev* **16**, 27-32 (2002).

40. Rosen, E.D., *et al.* C/EBPalpha induces adipogenesis through PPARgamma: a unified pathway. *Genes Dev* **16**, 22-26 (2002).

41. van der Meer, D.L., *et al.* Profiling of promoter occupancy by PPARalpha in human hepatoma cells via ChIP-chip analysis. *Nucleic Acids Res* **38**, 2839-2850 (2010).

42. Rosen, E.D. & Spiegelman, B.M. PPARgamma : a nuclear regulator of metabolism, differentiation, and cell growth. *J Biol Chem* **276**, 37731-37734 (2001).

43. Patsouris, D., *et al.* PPARalpha governs glycerol metabolism. *J Clin Invest* **114**, 94-103 (2004).

44. Martin, G., Schoonjans, K., Lefebvre, A.M., Staels, B. & Auwerx, J. Coordinate regulation of the expression of the fatty acid transport protein and acyl-CoA synthetase genes by PPARalpha and PPARgamma activators. *J Biol Chem* **272**, 28210-28217 (1997).

45. Haemmerle, G., *et al.* ATGL-mediated fat catabolism regulates cardiac mitochondrial function via PPAR-alpha and PGC-1. *Nat Med* **17**, 1076-1085 (2011).

46. Tontonoz, P. & Spiegelman, B.M. Fat and beyond: the diverse biology of PPARgamma. *Annu Rev Biochem* **77**, 289-312 (2008).

47. Ailhaud, G., Grimaldi, P. & Negrel, R. Cellular and molecular aspects of adipose tissue development. *Annu Rev Nutr* **12**, 207-233 (1992).

48. Chen, F., Law, S.W. & O'Malley, B.W. Identification of two mPPAR related receptors and evidence for the existence of five subfamily members. *Biochem Biophys Res Commun* **196**, 671-677 (1993).

49. Christy, R.J., *et al.* Differentiation-induced gene expression in 3T3-L1 preadipocytes: CCAAT/enhancer binding protein interacts with and activates the promoters of two adipocyte-specific genes. *Genes Dev* **3**, 1323-1335 (1989).

50. Schoonjans, K., *et al.* PPARalpha and PPARgamma activators direct a distinct tissue-specific transcriptional response via a PPRE in the lipoprotein lipase gene. *EMBO J* **15**, 5336-5348 (1996).

51. Mandard, S., *et al.* The direct peroxisome proliferator-activated receptor target fasting-induced adipose factor (FIAF/PGAR/ANGPTL4) is present in blood plasma as a truncated protein that is increased by fenofibrate treatment. *J Biol Chem* **279**, 34411-34420 (2004).

52. Steppan, C.M., *et al.* The hormone resistin links obesity to diabetes. *Nature* **409**, 307-312 (2001).

53. Hu, E., Liang, P. & Spiegelman, B.M. AdipoQ is a novel adipose-specific gene dysregulated in obesity. *J Biol Chem* **271**, 10697-10703 (1996).

54. Zimmermann, R., *et al.* Fat mobilization in adipose tissue is promoted by adipose triglyceride lipase. *Science* **306**, 1383-1386 (2004).

55. Haemmerle, G., *et al.* Defective lipolysis and altered energy metabolism in mice lacking adipose triglyceride lipase. *Science* **312**, 734-737 (2006).

56. Fredrikson, G., Tornqvist, H. & Belfrage, P. Hormone-sensitive lipase and monoacylglycerol lipase are both required for complete degradation of adipocyte triacylglycerol. *Biochim Biophys Acta* **876**, 288-293 (1986).

57. Lass, A., Zimmermann, R., Oberer, M. & Zechner, R. Lipolysis - a highly regulated multi-enzyme complex mediates the catabolism of cellular fat stores. *Prog Lipid Res* **50**, 14-27 (2011).

58. Bezaire, V., *et al.* Contribution of adipose triglyceride lipase and hormone-sensitive lipase to lipolysis in hMADS adipocytes. *J Biol Chem* **284**, 18282-18291 (2009).

59. Haemmerle, G., *et al.* Hormone-sensitive lipase deficiency in mice changes the plasma lipid profile by affecting the tissue-specific expression pattern of lipoprotein lipase in adipose tissue and muscle. *J Biol Chem* **277**, 12946-12952 (2002).

60. Fischer, J., *et al.* The gene encoding adipose triglyceride lipase (PNPLA2) is mutated in neutral lipid storage disease with myopathy. *Nat Genet* **39**, 28-30 (2007).

61. Schweiger, M., *et al.* The C-terminal region of human adipose triglyceride lipase affects enzyme activity and lipid droplet binding. *J Biol Chem* **283**, 17211-17220 (2008).

62. Dessen, A., *et al.* Crystal structure of human cytosolic phospholipase A2 reveals a novel topology and catalytic mechanism. *Cell* **97**, 349-360 (1999).

63. Rydel, T.J., *et al.* The crystal structure, mutagenesis, and activity studies reveal that patatin is a lipid acyl hydrolase with a Ser-Asp catalytic dyad. *Biochemistry* **42**, 6696-6708 (2003).

64. Shewry, P.R. Tuber storage proteins. *Ann Bot* **91**, 755-769 (2003).

65. Zechner, R., Kienesberger, P.C., Haemmerle, G., Zimmermann, R. & Lass, A. Adipose triglyceride lipase and the lipolytic catabolism of cellular fat stores. *J Lipid Res* **50**, 3-21 (2009).

66. Lu, X., Yang, X. & Liu, J. Differential control of ATGL-mediated lipid droplet degradation by CGI-58 and G0S2. *Cell Cycle* **9**, 2719-2725 (2010).

67. Raben, D.M. & Baldassare, J.J. A new lipase in regulating lipid mobilization: hormone-sensitive lipase is not alone. *Trends Endocrinol Metab* **16**, 35-36 (2005).

68. Lass, A., *et al.* Adipose triglyceride lipase-mediated lipolysis of cellular fat stores is activated by CGI-58 and defective in Chanarin-Dorfman Syndrome. *Cell Metab* **3**, 309-319 (2006).

69. Radner, F.P., *et al.* Growth retardation, impaired triacylglycerol catabolism, hepatic steatosis, and lethal skin barrier defect in mice lacking comparative gene identification-58 (CGI-58). *J Biol Chem* **285**, 7300-7311 (2010).

70. Cornaciu, I., *et al.* The minimal domain of adipose triglyceride lipase (ATGL) ranges until leucine 254 and can be activated and inhibited by CGI-58 and G0S2, respectively. *PLoS One* **6**, e26349 (2011).

71. Schweiger, M., Lass, A., Zimmermann, R., Eichmann, T.O. & Zechner, R. Neutral lipid storage disease: genetic disorders caused by mutations in adipose triglyceride lipase/PNPLA2 or CGI-58/ABHD5. *Am J Physiol Endocrinol Metab* **297**, E289-296 (2009).

72. Gruber, A., *et al.* The N-terminal region of comparative gene identification-58 (CGI-58) is important for lipid droplet binding and activation of adipose triglyceride lipase. *J Biol Chem* **285**, 12289-12298 (2010).

73. Huttlin, E.L., *et al.* A tissue-specific atlas of mouse protein phosphorylation and expression. *Cell* **143**, 1174-1189 (2010).

74. Mancuso, D.J., *et al.* Complex transcriptional and translational regulation of iPLAgamma resulting in multiple gene products containing dual competing sites for mitochondrial or peroxisomal localization. *Eur J Biochem* **271**, 4709-4724 (2004).

75. Chung, C., *et al.* Anti-angiogenic pigment epithelium-derived factor regulates hepatocyte triglyceride content through adipose triglyceride lipase (ATGL). *J Hepatol* **48**, 471-478 (2008).

76. Notari, L., *et al.* Identification of a lipase-linked cell membrane receptor for pigment epithelium-derived factor. *J Biol Chem* **281**, 38022-38037 (2006).

77. Zimmermann, R., Lass, A., Haemmerle, G. & Zechner, R. Fate of fat: the role of adipose triglyceride lipase in lipolysis. *Biochim Biophys Acta* **1791**, 494-500 (2009).

78. Schweiger, M., *et al.* G0/G1 switch gene-2 regulates human adipocyte lipolysis by affecting activity and localization of adipose triglyceride lipase. *J Lipid Res* **53**, 2307-2317 (2012).

79. Nielsen, T.S., *et al.* Reduced mRNA and protein expression of perilipin A and G0/G1 switch gene 2 (G0S2) in human adipose tissue in poorly controlled type 2 diabetes. *J Clin Endocrinol Metab* **97**, E1348-1352 (2012).

80. Oh, S.A., Suh, Y., Pang, M.G. & Lee, K. Cloning of avian G(0)/G(1) switch gene 2 genes and developmental and nutritional regulation of G(0)/G(1) switch gene 2 in chicken adipose tissue. *J Anim Sci* **89**, 367-375 (2011).

81. Zeng, F.*, et al.* Complementary deoxyribonucleic acid cloning of avian G0/G1 switch gene 2, and its expression and association with production traits in chicken. *Poult Sci* **90**, 1548-1554 (2011).

82. Yang, X., Zhang, X., Heckmann, B.L., Lu, X. & Liu, J. Relative contribution of adipose triglyceride lipase and hormone-sensitive lipase to tumor necrosis factor-alpha (TNF-alpha)-induced lipolysis in adipocytes. *J Biol Chem* **286**, 40477-40485 (2011).

83. Wueest, S., Yang, X., Liu, J., Schoenle, E.J. & Konrad, D. Inverse regulation of basal lipolysis in perigonadal and mesenteric fat depots in mice. *Am J Physiol Endocrinol Metab* **302**, E153-160 (2012).

84. Serr, J.*, et al.* Acute up-regulation of adipose triglyceride lipase and release of non-esterified fatty acids by dexamethasone in chicken adipose tissue. *Lipids* **46**, 813-820 (2011).

85. Brasaemle, D.L. Lipolysis control: the plot thickens. *Cell Metab* **11**, 173-174 (2010).

86. Ahmadian, M.*, et al.* Adipose overexpression of desnutrin promotes fatty acid use and attenuates diet-induced obesity. *Diabetes* **58**, 855-866 (2009).

87. Kershaw, E.E.*, et al.* Adipose triglyceride lipase: function, regulation by insulin, and comparison with adiponutrin. *Diabetes* **55**, 148-157 (2006).

88. Smirnova, E.*, et al.* ATGL has a key role in lipid droplet/adiposome degradation in mammalian cells. *EMBO Rep* **7**, 106-113 (2006).

89. Miyoshi, H.*, et al.* Control of adipose triglyceride lipase action by serine 517 of perilipin A globally regulates protein kinase A-stimulated lipolysis in adipocytes. *J Biol Chem* **282**, 996-1002 (2007).

90. Lefevre, C.*, et al.* Mutations in CGI-58, the gene encoding a new protein of the esterase/lipase/thioesterase subfamily, in Chanarin-Dorfman syndrome. *Am J Hum Genet* **69**, 1002-1012 (2001).

91. Srinivasan, R., Hadzic, N., Fischer, J. & Knisely, A.S. Steatohepatitis and unsuspected micronodular cirrhosis in Dorfman-Chanarin syndrome with documented ABHD5 mutation. *J Pediatr* **144**, 662-665 (2004).

92. Schleinitz, N.*, et al.* Two new mutations of the ABHD5 gene in a new adult case of Chanarin Dorfman syndrome: an uncommon lipid storage disease. *Arch Dermatol* **141**, 798-800 (2005).

93. Pujol, R.M.*, et al.* Erythrokeratoderma variabilis-like ichthyosis in Chanarin-Dorfman syndrome. *Br J Dermatol* **153**, 838-841 (2005).

94. Couturier, J., Patel, S.G., Iyer, D., Balasubramanyam, A. & Lewis, D.E. Human monocytes accelerate proliferation and blunt differentiation of preadipocytes in association with suppression of C/EBPAlpha mRNA. *Obesity (Silver Spring)* **20**,

253-262 (2012).

95. Yoon, I.K., *et al.* Exploration of replicative senescence-associated genes in human dermal fibroblasts by cDNA microarray technology. *Exp Gerontol* **39**, 1369-1378 (2004).

96. Koczan, D., *et al.* Gene expression profiling of peripheral blood mononuclear leukocytes from psoriasis patients identifies new immune regulatory molecules. *Eur J Dermatol* **15**, 251-257 (2005).

97. Colmegna, I., *et al.* Defective proliferative capacity and accelerated telomeric loss of hematopoietic progenitor cells in rheumatoid arthritis. *Arthritis Rheum* **58**, 990-1000 (2008).

98. Zhang, K., Zhang, R., Li, X., Yin, G. & Niu, X. Promoter methylation status of p15 and p21 genes in HPP-CFCs of bone marrow of patients with psoriasis. *Eur J Dermatol* **19**, 141-146 (2009).

99. Verner, J., *et al.* Gene expression profiling of acute graft-vs-host disease after hematopoietic stem cell transplantation. *Exp Hematol* **40**, 899-905 e895 (2012).

100. Shteyer, E., Liao, Y., Muglia, L.J., Hruz, P.W. & Rudnick, D.A. Disruption of hepatic adipogenesis is associated with impaired liver regeneration in mice. *Hepatology* **40**, 1322-1332 (2004).

101. Fernandez, M.A., *et al.* Caveolin-1 is essential for liver regeneration. *Science* **313**, 1628-1632 (2006).

102. Brasaemle, D.L. Cell biology. A metabolic push to proliferate. *Science* **313**, 1581-1582 (2006).

103. Farrell, G.C. Probing Prometheus: fat fueling the fire? *Hepatology* **40**, 1252-1255 (2004).

104. Yang, S.Q., Lin, H.Z., Mandal, A.K., Huang, J. & Diehl, A.M. Disrupted signaling and inhibited regeneration in obese mice with fatty livers: implications for nonalcoholic fatty liver disease pathophysiology. *Hepatology* **34**, 694-706 (2001).

105. Newberry, E.P., *et al.* Altered hepatic triglyceride content after partial hepatectomy without impaired liver regeneration in multiple murine genetic models. *Hepatology* **48**, 1097-1105 (2008).

106. Vilchez, C.A., Sadnik, I.L. & Bade, E.G. Influence of starvation on liver regeneration in the mouse. *Naturwissenschaften* **55**, 392-393 (1968).

107. Leduc, E.H. Mitotic activity in the liver of the mouse during inanition followed by refeeding with different levels of protein. *Am J Anat* **84**, 397-429 (1949).

108. Kuhn, R., Schwenk, F., Aguet, M. & Rajewsky, K. Inducible gene targeting in mice. *Science* **269**, 1427-1429 (1995).

109. Stacey, D.H., Hanson, S.E., Lahvis, G., Gutowski, K.A. & Masters, K.S. In vitro adipogenic differentiation of preadipocytes varies with differentiation stimulus, culture dimensionality, and scaffold composition. *Tissue Eng Part A* **15**, 3389-3399 (2009).

110. Amri, E.Z., Teboul, L., Vannier, C., Grimaldi, P.A. & Ailhaud, G. Fatty acids regulate the expression of lipoprotein lipase gene and activity in preadipose and adipose cells. *Biochem J* **314 (Pt 2)**, 541-546 (1996).

111. Reid, B.N.*, et al.* Hepatic overexpression of hormone-sensitive lipase and adipose triglyceride lipase promotes fatty acid oxidation, stimulates direct release of free fatty acids, and ameliorates steatosis. *J Biol Chem* **283**, 13087-13099 (2008).

112. Villena, J.A., Roy, S., Sarkadi-Nagy, E., Kim, K.H. & Sul, H.S. Desnutrin, an adipocyte gene encoding a novel patatin domain-containing protein, is induced by fasting and glucocorticoids: ectopic expression of desnutrin increases triglyceride hydrolysis. *J Biol Chem* **279**, 47066-47075 (2004).

113. Jeffrey, P.D.*, et al.* Mechanism of CDK activation revealed by the structure of a cyclinA-CDK2 complex. *Nature* **376**, 313-320 (1995).

114. Woo, R.A. & Poon, R.Y. Cyclin-dependent kinases and S phase control in mammalian cells. *Cell Cycle* **2**, 316-324 (2003).

115. Poon, R.Y., Jiang, W., Toyoshima, H. & Hunter, T. Cyclin-dependent kinases are inactivated by a combination of p21 and Thr-14/Tyr-15 phosphorylation after UV-induced DNA damage. *J Biol Chem* **271**, 13283-13291 (1996).

116. Lehman, J.J.*, et al.* Peroxisome proliferator-activated receptor gamma coactivator-1 promotes cardiac mitochondrial biogenesis. *J Clin Invest* **106**, 847-856 (2000).

117. Puigserver, P.*, et al.* A cold-inducible coactivator of nuclear receptors linked to adaptive thermogenesis. *Cell* **92**, 829-839 (1998).

118. Rowe, G.C., Jiang, A. & Arany, Z. PGC-1 coactivators in cardiac development and disease. *Circ Res* **107**, 825-838 (2010).

119. Ong, K.T., Mashek, M.T., Bu, S.Y., Greenberg, A.S. & Mashek, D.G. Adipose triglyceride lipase is a major hepatic lipase that regulates triacylglycerol turnover and fatty acid signaling and partitioning. *Hepatology* **53**, 116-126 (2011).

120. Wu, J.W.*, et al.* Deficiency of liver adipose triglyceride lipase in mice causes progressive hepatic steatosis. *Hepatology* **54**, 122-132 (2011).

121. Peyot, M.L.*, et al.* Adipose triglyceride lipase is implicated in fuel- and non-fuel-stimulated insulin secretion. *J Biol Chem* **284**, 16848-16859 (2009).

122. Kim, J.Y., Tillison, K., Lee, J.H., Rearick, D.A. & Smas, C.M. The adipose tissue triglyceride lipase ATGL/PNPLA2 is downregulated by insulin and TNF-alpha in 3T3-L1 adipocytes and is a target for transactivation by PPARgamma. *Am J Physiol Endocrinol Metab* **291**, E115-127 (2006).

123. Lake, A.C.*, et al.* Expression, regulation, and triglyceride hydrolase activity of Adiponutrin family members. *J Lipid Res* **46**, 2477-2487 (2005).

124. Kurat, C.F.*, et al.* Cdk1/Cdc28-dependent activation of the major triacylglycerol lipase Tgl4 in yeast links lipolysis to cell-cycle progression. *Mol Cell* **33**, 53-63 (2009).

125. Futcher, B. TgI4 lipase: a big fat target for cell-cycle entry. *Mol Cell* **33**, 143-144 (2009).

126. Cairns, R.A., Harris, I.S. & Mak, T.W. Regulation of cancer cell metabolism. *Nat Rev Cancer* **11**, 85-95 (2011).

127. Buchakjian, M.R. & Kornbluth, S. The engine driving the ship: metabolic steering of cell proliferation and death. *Nat Rev Mol Cell Biol* **11**, 715-727 (2010).

128. Fritz, V. & Fajas, L. Metabolism and proliferation share common regulatory pathways in cancer cells. *Oncogene* **29**, 4369-4377 (2010).

129. Aguilar, V. & Fajas, L. Cycling through metabolism. *EMBO Mol Med* **2**, 338-348 (2010).

130. Storck, S., Shukla, M., Dimitrov, S. & Bouvet, P. Functions of the histone chaperone nucleolin in diseases. *Subcell Biochem* **41**, 125-144 (2007).

131. Mongelard, F. & Bouvet, P. Nucleolin: a multiFACeTed protein. *Trends Cell Biol* **17**, 80-86 (2007).

132. Fahling, M., *et al.* Role of nucleolin in posttranscriptional control of MMP-9 expression. *Biochim Biophys Acta* **1731**, 32-40 (2005).

133. Otake, Y., *et al.* Overexpression of nucleolin in chronic lymphocytic leukemia cells induces stabilization of bcl2 mRNA. *Blood* **109**, 3069-3075 (2007).

134. Abdelmohsen, K., *et al.* Enhanced translation by Nucleolin via G-rich elements in coding and non-coding regions of target mRNAs. *Nucleic Acids Res* **39**, 8513-8530 (2011).

135. Heckmann, B.L., Zhang, X., Xie, X. & Liu, J. The G0/G1 switch gene 2 (G0S2): Regulating metabolism and beyond. *Biochim Biophys Acta* **1831**, 276-281 (2012).

136. Kersten, S. Mechanisms of nutritional and hormonal regulation of lipogenesis. *EMBO Rep* **2**, 282-286 (2001).

137. Sharara-Chami, R.I., *et al.* Epinephrine deficiency results in intact glucose counter-regulation, severe hepatic steatosis and possible defective autophagy in fasting mice. *Int J Biochem Cell Biol* **44**, 905-913 (2012).

138. Zechner, R. & Madeo, F. Cell biology: Another way to get rid of fat. *Nature* **458**, 1118-1119 (2009).

ACKNOWLEDGEMENTS

For privacy reason this part has been deleted

ACKNOWLEDGEMENTS

For privacy reason this part has been deleted

Curriculum Vitae

For privacy reason this part has been deleted